

©Copyright [2015]

[Nitish Sanjay Hirve]

Thermodynamic analysis of a Stirling engine using
second order isothermal and adiabatic models for
application in micropower generation system.

Nitish Sanjay Hirve

A thesis submitted in partial fulfillment of the
requirements for the degree of
Master of Science in Mechanical Engineering
University of Washington

2015

Committee:

Brian C. Fabien

John C. Kramlich

Igor Novosselov

Program Authorized to Offer Degree:

Mechanical Engineering

University of Washington

Abstract

Thermodynamic analysis of a Stirling engine using second order isothermal and adiabatic models for application in micropower generation system.

Nitish S Hirve

Chair of the Supervisory Committee:

Prof. Brian Fabien

Department of Mechanical Engineering

This work analyzes a Stirling cycle thermodynamically by breaking it down into different control volumes. A second order analysis has been performed and coded using Matlab as the platform. This code can be used to design a Stirling engine to get required power output and efficiency. The practical output will however be always less than that predicted by the code since it also depends on how well the engine has been machined. The closer the tolerances, the closer the output will get to that predicted by the code.

Besides designing a Stirling engine, the code can also be used to optimize the compression ratio and other parameters of the engine by performing simple edits.

University of Washington

Graduate School

This is to certify that I have examined this copy of a master's thesis by Nitish Sanjay Hirve and have found that it is complete and satisfactory in all respects, and that any and all revisions required by the final examining committee have been made.

Committee Members:

Brian C. Fabien

John C. Kramlich

Igor Novosselov

Date: _____

In presenting this thesis in partial fulfillment of the requirements for a Master's degree at the University of Washington, I agree that the Library shall make its copies freely available for inspection. I further agree that extensive copying of this thesis is allowable only for scholarly purposes, consistent with "fair use" as prescribed in the

U.S. Copyright Law. Any other reproduction for any purpose or by any means shall not be allowed without my written permission.

Signature: _____

Date: _____

CONTENTS

Chapter 1 – Energy today and related problems	1
Energy consumption pattern of the planet and associated problems	1
The need for micro-grid	5
The need for energy efficiency	6
Stirling system as an efficient, micro-grid standalone system.....	7
Chapter 2 – Literature review	10
Introduction to the Stirling cycle and Stirling engines	10
Introduction to fluidized bed combustors	18
Schematic of the co-generation system	23
Graphite foam.....	25
Chapter 3 – Thermodynamics analysis of the Stirling cycle using Matlab...	27
Ideal cycle analysis	30
Isothermal analysis of the Stirling cycle	35
Adiabatic analysis of the Stirling cycle	47
Chapter 4 – GPU-3 engine analysis and code validation.....	64
Comparison of GPU-3 results from code with published work	71
Compression ratio optimization of the GPU-3 Stirling engine.	82
Manufacturing of the free piston prototype	97

Bibliography	101
Appendix	103
Matlab program for isothermal analysis	103
Matlab code for adiabatic analysis	109

LIST OF FIGURES

FIGURE 1 PERCENTAGE OF MICROPOWER AND NUCLEAR POWER ENTERING THE GRID ..6	6
FIGURE 2: T-S DIAGRAM OF AN IDEAL STIRLING CYCLE	11
FIGURE 3: P-V DIAGRAM OF AN IDEAL STIRLING CYCLE	11
FIGURE 4: THE ALPHA CONFIGURATION STIRLING ENGINE	13
FIGURE 5: THE BETA TYPE STIRLING CONFIGURATION	15
FIGURE 6: THE GAMMA TYPE STIRLING ENGINE.....	16
FIGURE 7: THE FREE PISTON TYPE STIRLING ENGINE.....	17
FIGURE 8: FLUIDIZED BED COMBUSTOR SCHEMATIC.....	19
FIGURE 9: COST OF FBC TECHNOLOGY WITH MATURITY.....	20
FIGURE 10: EFFECT OF MOISTURE CONTENT ON HEATING VALUE	21
FIGURE 11: SCHEMATIC OF THE CO-GENERATION SYSTEM.....	23
FIGURE 12: CONTROL VOLUME DISTRIBUTION FOR ISOTHERMAL ANALYSIS.....	35
FIGURE 13: CONTROL VOLUME DISTRIBUTION FOR ADIABATIC ANALYSIS.....	50
FIGURE 14: ENERGY BALANCE FOR HOT END VOLUMES ONLY	56
FIGURE 15: ENERGY BALANCE FOR THE CONTROL VOLUMES	57
FIGURE 16: FLOWCHART FOR SECOND ORDER ANALYSIS	58
FIGURE 17: CONSTRUCTION OF GPU-3 ENGINE	65
FIGURE 18: SPECIFICATIONS FOR GPU-3 ENGINE.....	66
FIGURE 19: VOLUME VARIATION DURING CYCLE.....	67
FIGURE 20: PRESSURE VARIATION DURING CYCLE.....	68
FIGURE 21: PV DIAGRAM FOR THE GPU-3 ENGINE	69

FIGURE 22: TEMPERATURE VARIATION FOR GPU-3 DURING CYCLE	69
FIGURE 23: MASS FLOW IN CONTROL VOLUMES FOR GPU-3 DURING CYCLE	70
FIGURE 24: MASS VARIATION IN CONTROL VOLUMES FOR GPU-3 DURING CYCLE.....	70
FIGURE 25: INSTANTANEOUS WORK FOR GPU-3 DURING CYCLE	70
FIGURE 26: POWER OUTPUT COMPARISON AT 2.76MPA	71
FIGURE 27: POWER OUTPUT COMPARISON AT 2.76MPA	72
FIGURE 29: POWER OUTPUT COMPARISON AT 5.52MPA	74
FIGURE 28: POWER OUTPUT COMPARISON AT 5.52MPA	74
FIGURE 30: POWER OUTPUT PUBLISHED BY NASA.....	75
FIGURE 31: POWER OUTPUT USING COMBINED ANALYSIS	76
FIGURE 32: MECHANICAL LOSS VALUE FOR GPU-3.....	77
FIGURE 33: POWER OUTPUT COMPARISON FOR COMBINED ANALYSIS	78
FIGURE 34: HEAT INPUT TO GPU-3 ENGINE.....	79
FIGURE 35: EFFICIENCY COMPARISON FOR GPU-3	80
FIGURE 36: EFFECT OF CLEARANCE VOLUME	81
FIGURE 37: COMPRESSION RATIO OPTIMIZATION FOR MAXIMUM EFFICIENCY	83
FIGURE 38: COMPRESSION RATIO OPTIMIZATION FOR MAXIMUM POWER OUTPUT	83
FIGURE 39: POWER OUTPUT AND EFFICIENCY VERSUS REGENERATOR EFFECTIVENESS	89
FIGURE 40: POWER AND EFFICIENCY VERSUS PHASE ANGLE.....	90
FIGURE 41: POWER AND EFFICIENCY VERSUS COMP. RATIO FOR VARIABLE L/D	92
FIGURE 42: POWER AND EFFICIENCY VERSUS CLEARANCE HEIGHT	94

FIGURE 43: WORK AND HEAT IN THE CYCLE VERSUS VOLUME PHASE ANGLE	95
FIGURE 44: WORK AND HEAT IN A CYCLE FOR GPU-3.....	96
FIGURE 51: DISPLACER AND POWER PISTON CHAMBERS	97
FIGURE 52: DISPLACER CHAMBER WITH REGENERATOR	98
FIGURE 53: WORKING PISTON CHAMBER WITH PROJECTIONS TO SUPPORT DISPLACER	99
FIGURE 54: FINAL ASSEMBLY OF THE FREE PISTON ENGINE.....	100

ACKNOWLEDGEMENTS

I would like to thank Prof. Brian Fabien without whose support this work would not have been possible. He constantly encouraged us and gave valuable inputs at every stage from conception to execution. I would like to thank my research partner Mr. Amrit Om Nayak who is crucial to the work and whose experience and brilliance helped transform a rough concept into a tangible system. I would like to thank Eamon and Veasna, shop masters at the mechanical engineering workshop for extending support at every stage and pro-actively helping us through the entire manufacturing stage. I wish to thank Prof. Kramlich and Prof. Novosselov for their valuable support and help.

Finally and most importantly I would like to thank my family for being the strongest support at all times.

Chapter 1 – Energy today and related problems

Energy consumption pattern of the planet and associated problems

Energy is definitely one of the basic necessities of the current century. Everything we are using, has at some point in its life cycle, or is still consuming energy in some form. To start with, we will take a quick look at some of the current energy statistics at the global level that will be relevant in the context of the discussion that follows. The data has been sourced from the 63rd edition of the BP statistical review of World Energy, June 2014 (1).

- 2.3% increase in global primary energy consumption.
- Emerging economies accounted for 80% of global increase in energy consumption.
- 3.0% growth in coal consumption.
- Total proved oil reserves at the end of 2013 sufficient to meet 53 years of global consumption.
- Renewable resources account for 5.3% of global power generation.
- 2.7% growth in natural gas consumption in USA compared to 1.1% globally.
- US natural gas reserves stand at 11.7 trillion cubic meters at the end of 2013 with a reserves to production ratio of 13.

- Much higher increase in biofuels production, percentagewise, in South America and Asia Pacific as compared to the rest of the world.

Just like any good thing, good quality energy comes at a cost. The higher the quality of energy, the higher its price. Electric current or electricity is one of the forms of energy that positions itself higher in the energy hierarchy. But electricity itself does not occur naturally and comes from some lower quality (read less useful) energy, most often thermal energy which is converted to electricity at a centralized power plant and then distributed through the grid network. The problem with thermal energy, other than the fact that it is not the best form of energy one can have, is that it is a large source of pollution of every kind. Conventionally we obtain thermal energy from combustion, among which carbon combustion is dominant. Hence the problem of CO₂ and other greenhouse gases. It is now a well-established fact that global warming due to greenhouse gases is going to be the greatest challenge before the human race in the current and next century. What presently makes it a very tough nut to crack is that, with current energy and environmental policies, market technologies available and favorable economic cost it is extremely difficult to slow down greenhouse gas emissions without affecting economic growth in developing countries.

Coal and oil are no doubt the current favorite energy sources. Their abundance, low production cost and high energy density make them a tempting choice. Research over the last few decades has given rise to numerous promising clean energy sources. Among these, solar energy, wind energy and nuclear energy are more popular, although biomass is catching up rapidly in some regions. Even if the energy we are using appears clean and non-polluting, at some point it has produced carbon emissions. Solar panels that are supposedly a clean energy source have produced carbon emissions during their manufacture. Thus no life cycle is 'carbon neutral' yet. The argument that biomass is a carbon neutral energy source is still under debate (2). So currently we have solutions that produce relatively less carbon emissions or fixed carbon emissions. Solar panels as discussed earlier produce carbon emissions only during its manufacture and installation and negligible thereafter. They can be said to produce fixed carbon emissions. An example of the energy source that produces relatively less carbon emissions is natural gas. Natural gas composition is almost entirely methane. One methane molecule has four hydrogen atoms and one carbon atom, compared to conventional coal which is almost entirely carbon. On combustion it will produce one CO₂ atom and four H₂O atom. Thus it produces relatively less carbon dioxide for the same amount of energy generated. Further USA has abundant natural gas resources and the recently developed combined cycle

technology which gives never before attained efficiencies for a power generation plant. If we combine the cleaner emissions and high conversion efficiency, it tremendously amplifies the value of natural gas as a clean fuel, provided it is available in sufficient quantities. Fortunately for US, it has enough natural gas to operate as clean fuel until the next generation of cleaner sources are available with economic and technical feasible. For countries which do not have sufficient natural gas reserves, other clean energy resources can be tapped into. Biomass energy is available on a large scale but clearly untapped in most agrarian economies due to lack of technology and/or required logistics. Some or all among solar, wind, tidal and geothermal energy sources are available to most countries on the planet. These are clean energy sources, but again lack of technology and costs associated with implementation restrict their use. Also these resources are not concentrated and are available in fringes over a large area. Nuclear energy which is also supposedly clean, requires necessary technology which is most often a secret recipe restricted to a few and a high capital. Thus, availability (of natural gas) and nature (scattered nature of renewable sources) of availability, technological and economic hurdles in the use and implementation of clean resources currently favor the conventional polluting sources for satisfying energy needs.

The need for micro-grid

So far the magnitude of energy consumption, the ever increasing demand for energy, the associated problems with conventional energy sources and the hurdles in the implementation of clean energy have been presented. For sources other than natural gas, the primary issue seems to be scattered distribution, lack of technology (nuclear energy) and cost of implementation. A couple of these can be addressed through the implementation of micro-grid. Micro grid aims at decentralizing the presently dominating centralized power distribution systems. Many developing countries like India do not have sufficient grid connectivity leading to energy poverty. This failure to establish a sufficient grid network can be seen as a potential opportunity to implement micro grid networks. Off the grid standalone systems can be implemented in areas where solar, wind, geothermal or a combination of these are available. This saves the capital cost of establishing a grid network and also avoids transmission losses. Also the micro grid will be saved from power outages in the main grid. It can also help in better security and safety. It will ensure continuous uninterrupted power supply even during grid failure. By decentralizing power microgrids one can ensure that power reaches even remote parts of developing nations, where a large majority lacks basic access to electricity. With better reliability and ability to work in sync with renewable technologies, micro grid seems to have a bright future. Hence, independent

micropower generation systems shall gain significance in the near future. The following graph reproduced from the work (3) published by the Rocky Mountain Institute shows the percentage of electricity entering the main grid from micro grids over the past few years.

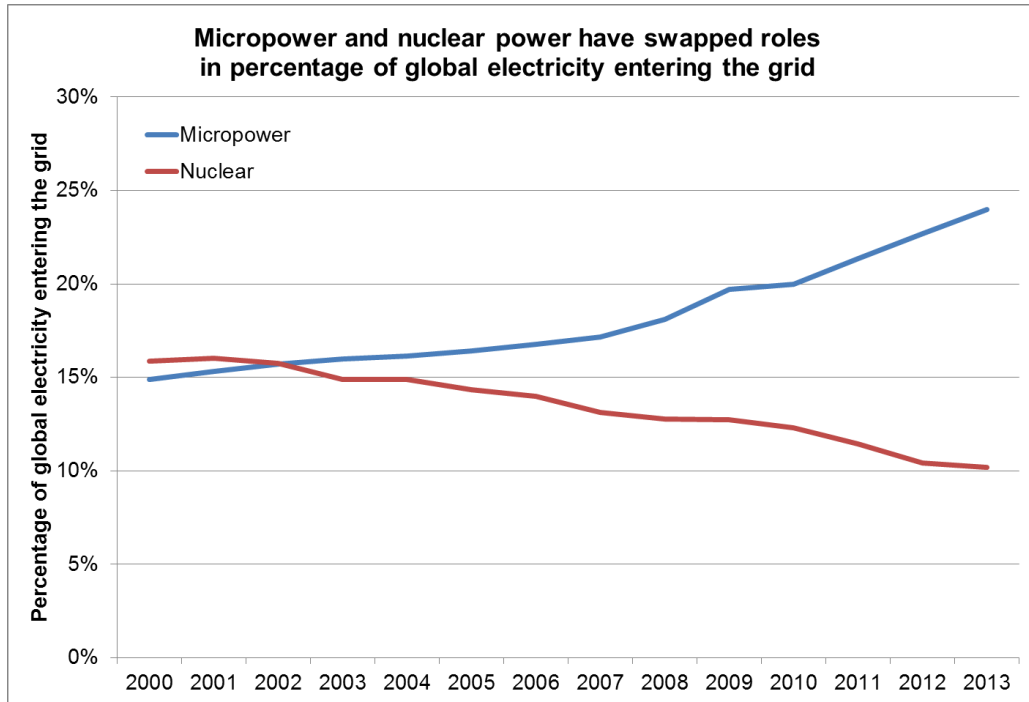


Figure 1 Percentage of micropower and nuclear power entering the grid

The need for energy efficiency

A penny saved is a penny earned. Similarly a kW of electricity saved is 3kW of thermal energy saved, considering efficiencies of the conversion systems. Energy is a multi-trillion dollar business worldwide and saving even a small percentage of energy means saving a few billion dollars. The average overall efficiency of a centralized power generation and

distribution should come to about 30% or lesser. The average Rankine cycle efficiency is about 37%, there are further losses in grid distribution, stepping down and then local distribution. If we consider the losses during the mining or extraction of coal and oil, this efficiency will reduce even more. Effectively only a small fraction of the energy source is left till it reaches the end user. Combined cycle power plants have higher efficiencies, but natural gas is not available in every region of the world. There is also a myth that energy efficiency comes with a cost and higher the efficiency required, higher is the capital investment. A detailed economic analysis by Amory Lovins in his book 'Reinventing Fire' shows that energy efficiency projects totally justify the investment and if carefully planned, can cost less than standard systems.

Stirling system as an efficient, micro-grid standalone system

Engines currently are classified into two types based on operation, internal combustion engines and external combustion engine. Stirling engines belong to the external combustion type. In a Stirling engine, we have the normal piston-cylinder arrangement as found in normal IC engines. A displacer is also a part of the engine in some configurations. The Stirling engine needs to be heated externally at its hot end and the cold end of the engine is supposed to be maintained at a lower temperature. More the temperature difference between the two ends of the engine, better is the

efficiency. In an alpha configuration of Stirling engine, the hot and cold ends are two separate cylinders which makes it easier to maintain a temperature differential, by avoiding heat conduction. In single cylinder Stirling engines, care should be taken to minimize conductive heat transfer across the cylinder walls and across the displacer. The main advantage of a Stirling engine lies in the very fact that it is an external combustion engine. Thus the fuel combusted to heat the engine can be anything. A Stirling engine can operate on any heat source providing with flexibility in our choice of fuel. This gives the opportunity to use multiple fuels for the same system depending on availability and cost factors. If a system is built, that generates power using a Stirling engine running on multiple clean fuels, at an economical cost and with minimum operational costs, it could change the face of most developing countries that have large regions with no access to power. These regions can be powered using a Stirling engine system. From one house, to an entire village, the Stirling engine system can be scaled depending on necessity. The fuel required for generating power can be provided locally through agricultural and animal waste. The benefit of fuel flexibility, economy of operation, high efficiency of Stirling engines make this option really attractive as against conventional diesel generators. This system can also be integrated with solar thermal to power during the day. A mix of solar thermal and biomass can be used to strike an economic balance for optimum performance. An integrated system

where a standalone power generation system involving a Stirling engine, works in sync with the fuel logistics will present itself as an ideal solution to the issue of lack of access to power.

Chapter 2 – Literature review

Introduction to the Stirling cycle and Stirling engines

A Stirling cycle is a regenerative thermodynamic cycle. Its ideal efficiency is equal to ideal Carnot efficiency. The ideal cycle has four processes including two isothermal and two isochoric processes.

The processes shown in the figure 2 and 3 are,

1-2: isothermal compression, heat transfer occurs from hot working fluid to cold surroundings at cold end of engine

2-3: constant volume heat addition to working fluid from the regenerator

3-4: isothermal expansion, heat transfer occurs from hot temperature source to working fluid at the hot end of engine

4-1: constant volume heat addition to the regenerator from the hot working fluid

It is assumed that the regeneration process is ideal, which is the regenerator gives back as much heat to the working fluid after the compression process, as it had absorbed after the expansion process. This shows to some extent the importance of a well performing regenerator section in the overall execution of the Stirling cycle. The importance of regeneration will further be highlighted eventually as the analysis proceeds and comparative studies are done using the analysis. The ideal Stirling

cycle has been represented on TS and PV diagrams below. They will help understand the nature of this cycle.

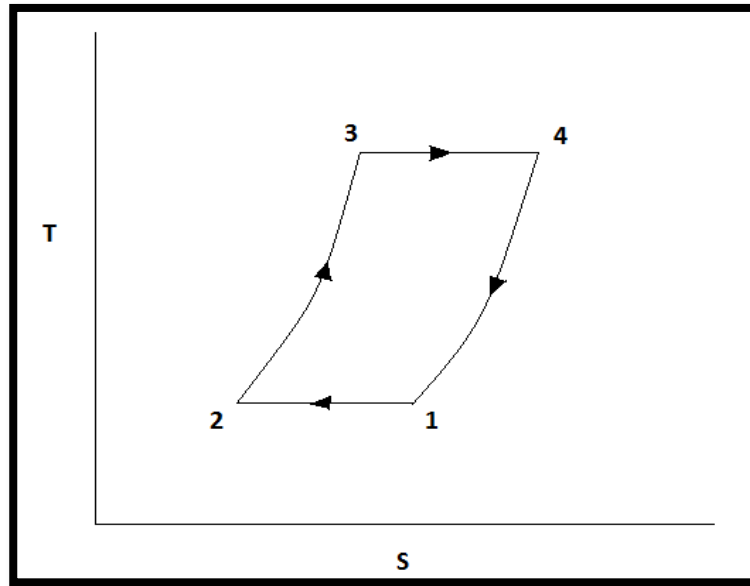


Figure 2: T-S diagram of an ideal Stirling cycle

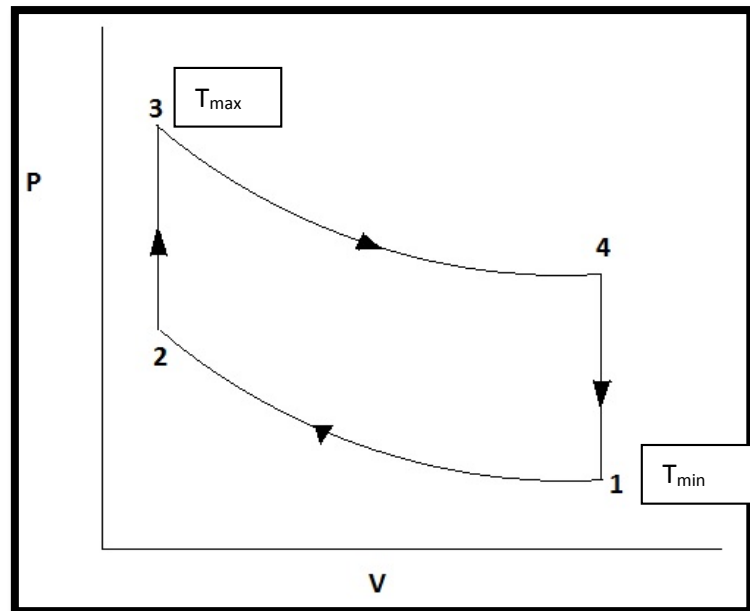


Figure 3: P-V diagram of an ideal Stirling cycle

The limiting efficiency for this cycle is the same as efficiency of a Carnot cycle working between the same temperature limits T1 and T2. The limiting efficiency will be evaluated as,

$$\eta = 1 - (T_{\min}/T_{\max})$$

where,

η =maximum possible efficiency

T_{\min} =lower temperature limit (engine cold end mean temperature of heat rejection)

T_{\max} =higher temperature limit (mean temperature of heat addition at hot end of engine)

Now for the engine if we assume the hot end engine temperature at 600°C and cold end engine temperature as 50°C, then the limiting efficiency of the engine will be,

$$\eta = 1 - (50 + 273) / (600 + 273) = 0.63 = \mathbf{63\%}$$

Of course this limit cannot be achieved due to inherent losses and irreversibility that will accompany every process involved in the engine operation. However, our target will be to maximize the efficiency as well as work output from the engine. Thermodynamics analysis of the cycle will point to the source of losses and help identify areas requiring

improvement. The two parameters, efficiency and work output, which will dominate the engine design, may sometimes be in conflict as we will see in the parametric study in the Chapter 4.

A Stirling engine is an external combustion engine. It is ideally a completely sealed engine with the working gas filled inside the engine. The engine is then heated from the outside at its hot end and heat is withdrawn from its cold end. The variations in the thermodynamic parameters of the working gas produces mechanical work which can be tapped. Many configurations of a Stirling engine have been developed over the years, but the popular ones are the alpha type Stirling engine, the beta type Stirling engine, the gamma type Stirling engine and the recently developed free piston Stirling engine. Each one of these has their unique advantages and disadvantages. The basic difference between each of these configurations is given below. The diagrams have been reproduced from the Ohio State University's mechanical engineering website.

The alpha type Stirling

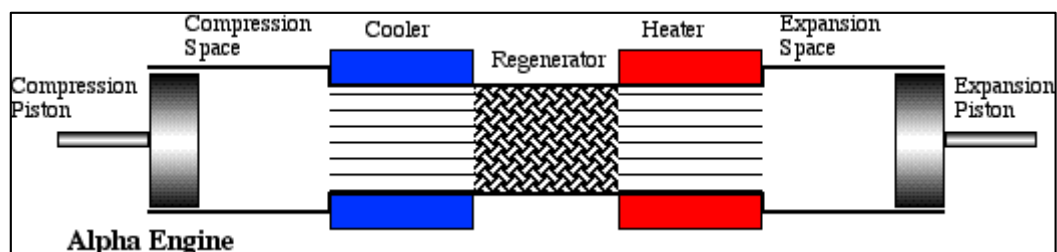


Figure 4: The alpha configuration Stirling engine

The alpha type Stirling has two separate cylinders connected through a path that also houses the regenerator. One of the cylinders is heated and becomes the hot end for the cycle. The other cylinder is cooled and becomes the cold end of the cycle. This cylinder may be air cooled, water cooled or any other coolant can be used depending of the feasibility of its use. The pistons of both cylinders are connected to a common crank through their respective connecting rods. A phase difference of about 90 degrees is maintained between the strokes of the two cylinders. The expansion process occurs in the hot cylinder and the compression process in the cold cylinder. The regenerator section acts as a thermal energy storage reservoir. Its job is to absorb as much heat as possible while the gas flows from the hot end towards the cold end, and return as much as possible while the gas travels from the cold end back to the hot end. It thus reduces the amount of heat that should be provided at the hot end and the amount of heat to be rejected at the cold end, thereby improving thermal efficiency of the engine. There are pressure losses when the working gas passes through the regenerator section as it obstructs the flow. Over the years, steel wool, aluminum wool, metal foams have been popularly used as regenerator material. For the proposed system, graphite foam is being considered as the regenerator material. More on this material has been presented in a later chapter.

The beta type Stirling

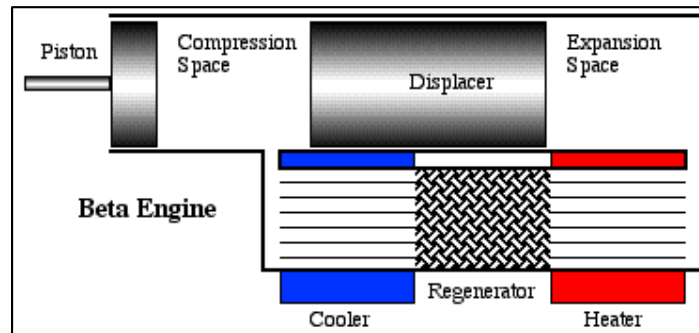


Figure 5: The beta type Stirling configuration

In this configuration, we have a displacer and a working piston, which are co-axial. The job of the displacer is to circulate the working fluid between the hot and cold ends, while absorbing minimum work from the cycle. Thus in a beta engine the work is produced by the working piston only, and the displacer is a volume separator/gas reciprocator. For a beta type Stirling, the hot and cold ends are present in the same cylinder and all the processes take place in this same cylinder. The reciprocating motion of the working piston varies the volume available inside the cylinder for the gas to occupy, and thereby varies the pressure inside the engine. The regenerator is usually placed circumferentially around the displacer for simple beta configurations and its function is the same as that in an alpha configuration. The working piston and displacer are connected to a common crank through their connecting rods. The co-axial nature of the piston and displacer make the connecting rod design slightly complicated.

So gas springs are used for displacers instead of a connecting rod. There are possibilities of losses due to heat being conducted from the hot end to the cold end, both being present in the same cylinder, through cylinder walls and across the displacer. This problem is not present in an alpha type. To avoid this the beta type engine displacers are generally long so that the conductive heat transfer loss called ‘shuttle losses’ are minimized.

The gamma type Stirling engine

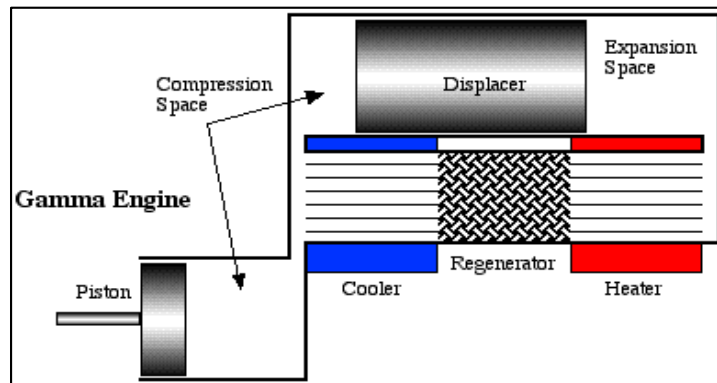


Figure 6: The gamma type Stirling engine

In this third configuration, the working piston and the displacer are present in the same cylinder but are not co-axial. The working piston and displacer are attached to a common crank. A complicated connecting rod design is avoided and the sizes of the displacer and working piston can easily be adjusted as required, unlike in a beta engine, where the diameters of the displacer and the working piston cannot have a large difference.

The free piston Stirling engine by William Beale. This image is reproduced from the Sunpower website. Sunpower is a free piston Stirling manufacturing company in Ohio. A published work by Seon Young Kim (4) for Sunpower gives a good understanding about the power generation capability of a free piston Stirling engine.

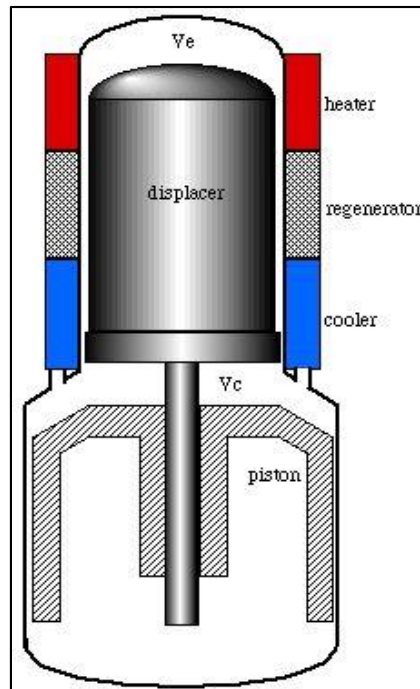


Figure 7: The free piston type Stirling engine

The previous three configurations were connected to a crank and carried side forces by the cylinder wall on the piston/displacer. A free piston is designed to reciprocate linearly without attachment to any crank and is 'free' from side forces. The free piston engine was designed by William Beale to be directly coupled with a linear alternator for power

generation. Instead of a conventional flywheel, gas springs, coil springs or membrane springs are used to sustain the engine cycle.

Introduction to fluidized bed combustors

As discussed previously an independent system generating micropower using a Stirling engine has multiple advantages. However to take advantage of the fact that a Stirling engine can run on multiple fuels, we need a system that can combust a variety of fuels efficiently. The fluidized bed combustion technology allows us to efficiently combust a wide variety of fuels. A fluidized bed combustor is a combustion chamber that has a sand bed. This sand bed is 'fluidized' by passing an air stream through it. The velocity of the air stream is crucial and decided if the fluidized bed is a bubbling bed type combustor or a circulating bed type combustor. The FBC gives a very high combustion efficiency of almost or close to 100%. It can burn most solid fuels efficiently, including coal, biomass, wood pellets and other solid waste. For solid fuels that contain moisture some drying might be necessary before they are fed into the FBC. The fluidized bed causes a rigorous mixing of fuel particles, thereby rapidly triggering the kinetics of combustion. It ensures that almost every fuel particle has combusted by thoroughly mixing the fuel particles and oxidizing air in the combustion chamber. The thermal efficiency of a boiler employing a

fluidized bed combustor can reach up to 92% depending on the quality of fuel used. Even for the low grade fuels the thermal efficiencies are quite good, most often above 82%. The FBC can also accommodate different fuel particle sizes. The figure below shows a fluidized bed combustor by TSK,

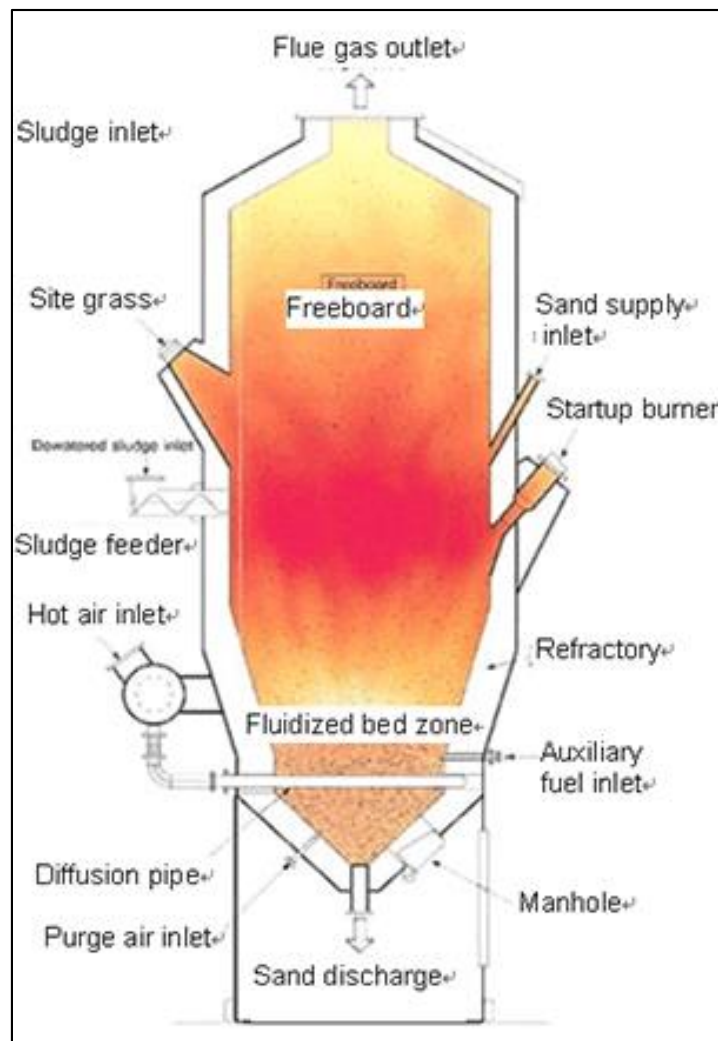


Figure 8: Fluidized bed combustor schematic

The important aspects that favor the use of FBC in the hybrid Stirling engine system is that it is a scalable technology and has matured over the years. Maturity of a technology brings down its cost to a great extent as can be seen from the following graph reproduced from the work by Joris Koorneef (5).

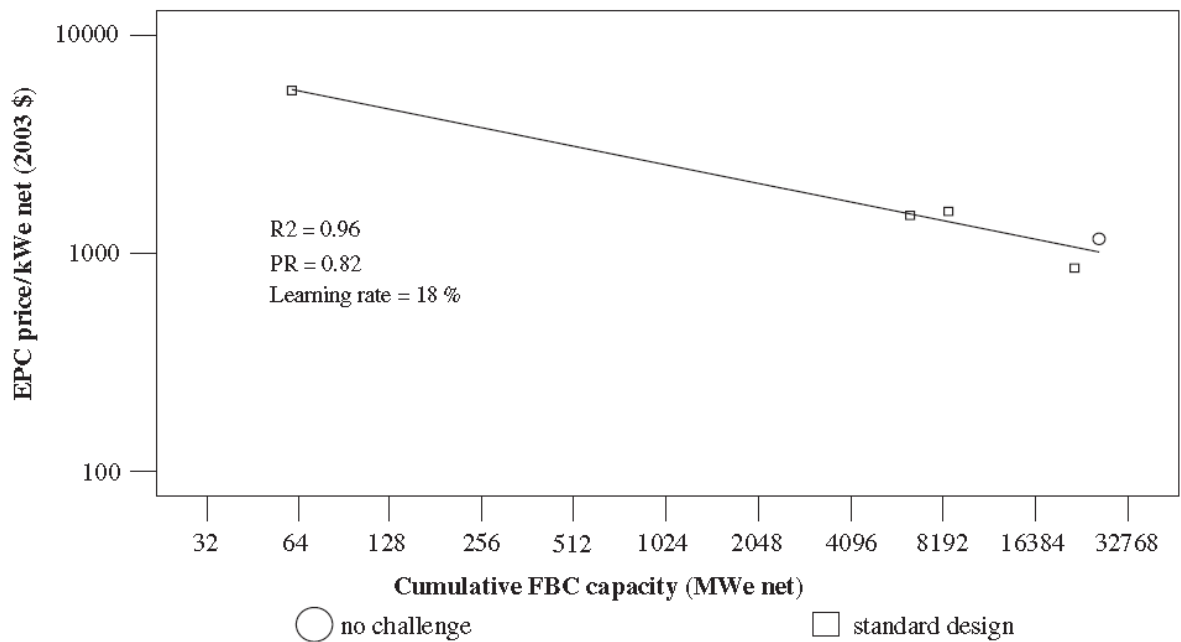


Figure 9: Cost of FBC technology with maturity

Though the fluidized bed looks like a very attractive option, there are some issues that need to be resolved before it becomes totally feasible for the co-generation system at the micro scale. The first issue is the disposal of the solid waste generated after combustion. A lot of solid waste is generated from low quality fuels which needs to be disposed appropriately. Also the cost of FBC increases as the quality of fuel

depreciates. Thus a minimum quality of fuel should be maintained to ensure that the system can be designed economically. The third issue is that some fuels have high water content and require drying. This asks for the addition of a separate fuel drying system, thereby increasing the total cost of the co-generation system. The drying of the fuel is crucial as it directly affects the calorific value one can get from the fuel. The figure below reproduced from the work by Rick Curkeet (6) shows the effect of moisture content on the heating value of wood.

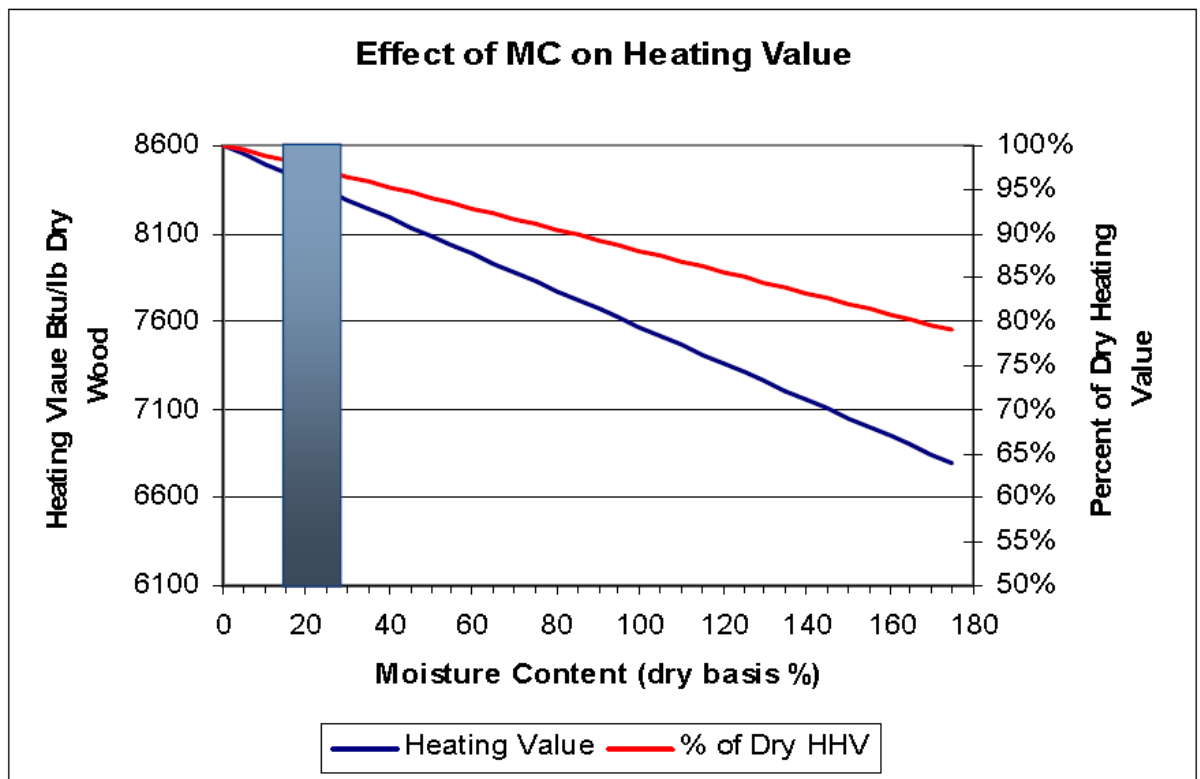


Figure 10: Effect of moisture content on heating value

Clearly drying the fuel will play an important role in deciding the thermal efficiency of a system. An extensive study and system for solid fuel and biomass drying has been prepared by Amrit Om Nayak and can be found in his work titled 'Holistic Modeling, Design & Analysis of Integrated Stirling and Auxiliary Clean Energy Systems for Combined Heat and Power Applications' (7). The government policies also play a crucial role in evaluating the viability of biomass as a fuel. This topic has been presented well in the work by Larry Mason (8).

Schematic of the co-generation system

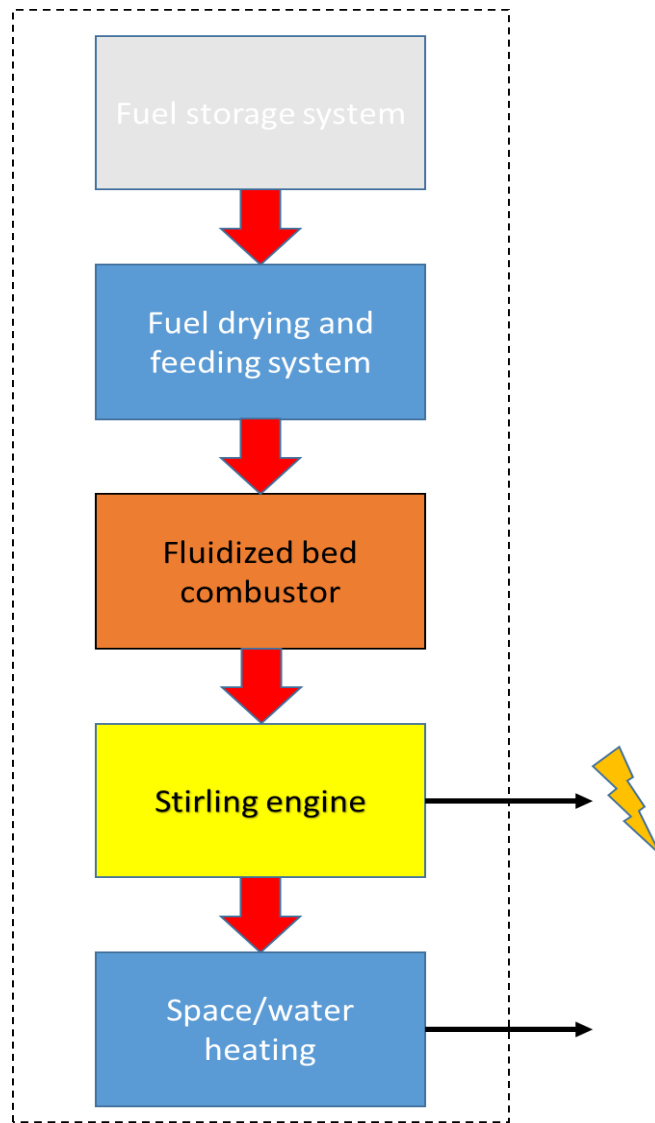


Figure 11: Schematic of the co-generation system

The cogeneration system is represented in the schematic above. A fuel storage system will the fuel to a moisture removal system, which can work on solar thermal energy. Next the dry fuel is then fed to the

fluidized bed combustor for combustion. The fuel drying system will control the rate of combustion and a supply fan with VFD will provide sufficient quantity of combustion air to the fluidized bed combustor. The hot flue gases generated will heat the hot end of the Stirling engine and the downstream will be used for space heating or producing hot water. Alternatively, the fuel can be gasified and the partially combusted flue gases can heat the Stirling engine and then be used for cooking purposes. Both gasification and combustion can be done in a single FBC if the amount of fuel and air can be controlled accurately. A small auxiliary system will be needed for startup. The Stirling engine is hooked up to an alternator to produce electricity at directly usable voltage levels. The downstream of a gasifier system can be used as cooking gas in villages and remote towns. The system can be made economically feasible by installing a common system for a large group of people rather than having individual systems. The additional cost of the fuel drying system can be justified by using the same drying system for moisture removal of food grains and other agricultural produce, thereby increasing their storage life. This will result in less wastage and improved productivity and the payback costs for the moisture removal system can be minimized. Besides the system operates on free solar thermal power, thereby economizing the operational costs.

Graphite foam

For years a lot of materials and configurations have been tested for the regenerator section of the Stirling engine. But there is no perfect solution to the problem yet. Clearly indicates the importance of the regenerator effectiveness and its effect on our desired output. Undoubtedly the regenerator is the most crucial section in the engine and its importance is second to none. In all analysis to be presented the regeneration is assumed to be perfect. What this actually means is that when the gas leaves the regenerator section and flows towards the hot end it will exit at the hot end heat exchanger temperature. Similarly when the gas exits the regenerator towards the cold end of the engine, it will exit at the cold end heat exchanger temperature. Now the problem is that this can never occur in real engines, no matter how much the efficiency of heat transfer in the regenerator is increased. There are many obstacles that prevent perfect regeneration from occurring. Firstly there is insufficient time for the heat transfer to occur. Next the heat transfer rate is limited by the thermal conductivity of the material used in the regenerator section. Lastly there is insufficient area of contact for heat transfer if we use metal wire mesh or similar structures. There is a problem of material stability at high operation temperatures of the engine. These are the few major problems associated with the regenerator section. However a possible solution to

these problems might be found in a newly invented non-traditional carbon foam, called 'graphite foam'. This material was invented by Dr. James Klett at the Oak Ridge National Laboratories (ORNL) and has some wonderful properties that are desirable for the regenerator. Some details regarding this material are given below, (9)

- 1) Formal name – High thermal conductivity, mesophase pitch-derived carbon foam. (9)
- 2) Density of 2.23 g/cm³. (9)
- 3) Bulk conductivity = 180 W/m-K. Conductivity of carbon fibers = 1600W/m-K. (9)
- 4) Low pressure drop
- 5) Stable at very high temperatures in oxygen free environment. Our working fluid is helium.
- 6) Excellent workability.
- 7) Porosity of 75%.

These properties make it a better candidate than the traditional wire mesh for use as regenerator material. Much improved output is expected by use of this material and it may prove to be the wonder material for Stirling engines.

Chapter 3 – Thermodynamics analysis of the Stirling cycle using Matlab

First-Order Analysis

First-order design methods are used for basic Stirling engine performance predictions while keeping calculations simple. Calculation of power output starts with an ideal analysis generally using the Beale number and equation. Correction factor is applied to this analysis to predict a better performance that is slightly more realistic.

These efficiency and power correction factors are determined from statistical data published. As a rule of thumb, the Stirling engine can achieve a performance of 0.6 times that predicted by an ideal adiabatic analysis. First order analyses are a quick way to estimate the overall size of an engine and its power output, but not very useful as detailed design tools for Stirling engines.

Second-Order Methods

A simplified cycle analysis is done to determine a basic power output and heat input. Different power losses are then subtracted from the basic power output, and heat losses are added to the heat input to get the effective performance values. Power losses include fluid and mechanical friction, heat transfer losses in cylinders and gas leakage past seals. Heat losses include shuttle losses, conduction and imperfect

regenerator loss. The effect of an imperfect regenerator has been covered in a later chapter in this report. Each of the energy loss calculated is considered independent of each other in the second order methods.

Isothermal analysis

This analysis is based on Schmidt isothermal cycle, which allows for sinusoidal volume variations. It is a slightly more realistic form of the ideal Stirling cycle. The gas in the expansion space is assumed to be at a constant temperature equal to the heat source temperature, and the gas in the compression space is assumed to be at a constant temperature equal to the heat sink temperature. The heat transfer coefficients are perfect/infinite for this analysis with zero temperature differential between the gas and the cylinder walls. Perfect regeneration is also. All heat input to the isothermal cycle occurs in the expansion space, and all heat output occurs in the compression space.

Adiabatic analysis

The adiabatic cycle assumes that the compression and expansion spaces are perfectly insulated. This is more realistic and adiabatic conditions can be safely assumed since the engines operate at high frequencies allowing little or no time for heat transfer in the working spaces. All heat input to the cycle occurs in the heater, and all heat

output occurs in the cooler. Gases leave the heater at the heat source temperature and are mixed perfectly as soon as they enter the expansion space. Similarly, gases leave the cooler at the heat sink temperature and are mixed perfectly as soon as they enter the compression space. In this case too, perfect regeneration is assumed.

Semi-adiabatic analysis

Semi-adiabatic cycles considers a nonzero, finite heat transfer coefficient between gas and the cylinder walls. The simplest semi-adiabatic cycle, first analyzed by Finkelstein, accounts for heat transfer in the expansion and compression spaces. The wall temperatures of these volumes are assumed to be constant with respect to time and equal to the heat source and heat sink temperatures, respectively. The heater, cooler, and regenerator are assumed perfect. The consideration of irreversible heat transfer losses across the temperature difference between the gas and the cylinder walls in the compression and expansion spaces causes the analysis to predict lower power and efficiency values than the previous two analysis.

An extensive analysis has also been presented in the work by Thombare and Verma (10).

Ideal cycle analysis

First a quick analysis of the ideal cycle is shown below.

The basic assumptions for an ideal Stirling cycle:

- a) Zero dead volume in engine.
- b) Uniform pressure throughout the cycle at any instant, that is, there is no pressure drop in any section of the engine. Viscous and frictional losses have been ignored using this assumption.
- c) Perfect regeneration. (The formal definition and significance of regenerator effectiveness will be covered in the parametric study section of the report).
- d) The cycle follows the ideal path for a Stirling thermodynamic cycle between two given temperature limits.
- e) Working fluid (which has not been specified till now) obeys ideal gas law.

Nomenclature for the analysis:

W = Work output, in J/cycle.

m = Mass of working fluid circulating in the cycle, in kg.

R = Gas constant for the working fluid, in J/kg-K.

T= Temperature during the corresponding process for which work is calculated, in K.

V= instantaneous volume in the cycle, in m³.

With these assumptions the work output per process in the cycle can be given by-

$W_1 = m R T \ln(V_2/V_1)$ for process 1-2, work done by an ideal gas in an isothermal process

$W_2 = m R T \ln(V_3/V_2) = 0$ for process 2-3, isochoric process

$W_3 = m R T \ln(V_4/V_3)$ for process 3-4, work done by an ideal gas in an isothermal process

$W_4 = m R T \ln(V_1/V_4) = 0$ for process 4-1

Thus, the total work output from one cycle will be-

$W = W_1 + W_2 + W_3 + W_4 = W_1 + W_3$ in J/cycle.

The heat input to the cycle will be-

$Q_{in} = m C_v (T_3 - T_2)$ in J/cycle.

Then the efficiency of the cycle will be-

$\eta = (W_1 + W_3) / Q_{in}$

The methodology for the thermodynamic analysis of a Stirling cycle remains the same irrespective of the type of Stirling engine being designed. This is because all configurations will follow the same thermodynamic cycle and only the dynamics of the engine will vary. Thus the analysis that will be developed in Matlab can be applied to any Stirling engine. This is useful since two options for building the system have been considered. The first one being a custom designed free piston Stirling engine and the second being converting an existing IC engine into an alpha type Stirling engine.

For the purpose of analysis, initially the thermodynamic analysis of the ideal Stirling cycle would be done, where we have two isothermal (expansion and compression) and two isochoric processes. Eventually we will modify the analysis so that the two isothermal processes (expansion and compression) in the cycle are now adiabatic. Further, the different engine parameters will be introduced in this analysis to see the variation in performance and output of the engine as these parameters vary. For the purpose of analysis methodology, the Stirling engine design guide (11) prepared by William Martini for NASA and DOE's office of vehicle and engine R&D has been referred. Solutions to the differential equations in adiabatic analysis have been referred from the paper by Jose Martinez (12). There are certain simplifying assumptions for the purpose of analysis and

these assumptions with their significance in the analysis is stated. Also, the nomenclature used for each of these analysis is also stated in their respective sections.

There are a variety of options available to work as a working fluid for Stirling engines. The working fluids that have seen extensively experimented with include air, carbon dioxide, nitrogen, helium and hydrogen. Among these helium and hydrogen prove to be the most promising in terms of power output and efficiencies. The power produced by the engine will depend to a large extent upon the heat absorbing capacity of the working gas at the hot end. The more heat the working gas can absorb at the hot end, the higher the power it can produce. Thus working fluid with higher specific heats will have the capability to produce more power, because they will absorb more heat per unit rise in temperature provided we have a good overall heat transfer co-efficient at the hot end to keep up with the rate of heat absorption by the working fluid. Obviously at the cold end, more heat will be rejected by working fluid with high specific heats for a given temperature drop. Hence efficient cooling is required at the cold end too.

The efficiency of a Stirling engine also depends largely on how well the regenerator section performs. A good regenerator will absorb as much heat as it can from the working fluid while the gas flows from the hot end to the

cold end, thereby reducing the cooling load at the cold end. On the other hand it will give back as much as it can to the working fluid while it travels back from the cold end to the hot end, thereby reducing the amount of heat that the hot end heat exchanger needs to impart to the working fluid.

The heat exchanger (hot end and cold end) effectiveness, the conductive, convective and radiative heat losses, viscous forces inside the engine will all play their respective part in making the engine inefficient. However the thermodynamic analysis will be isolated from heat transfer and viscous forces considerations for simplicity. We will consider only the state variables pressure, volume and temperature for the purpose of analysis.

Isothermal analysis of the Stirling cycle

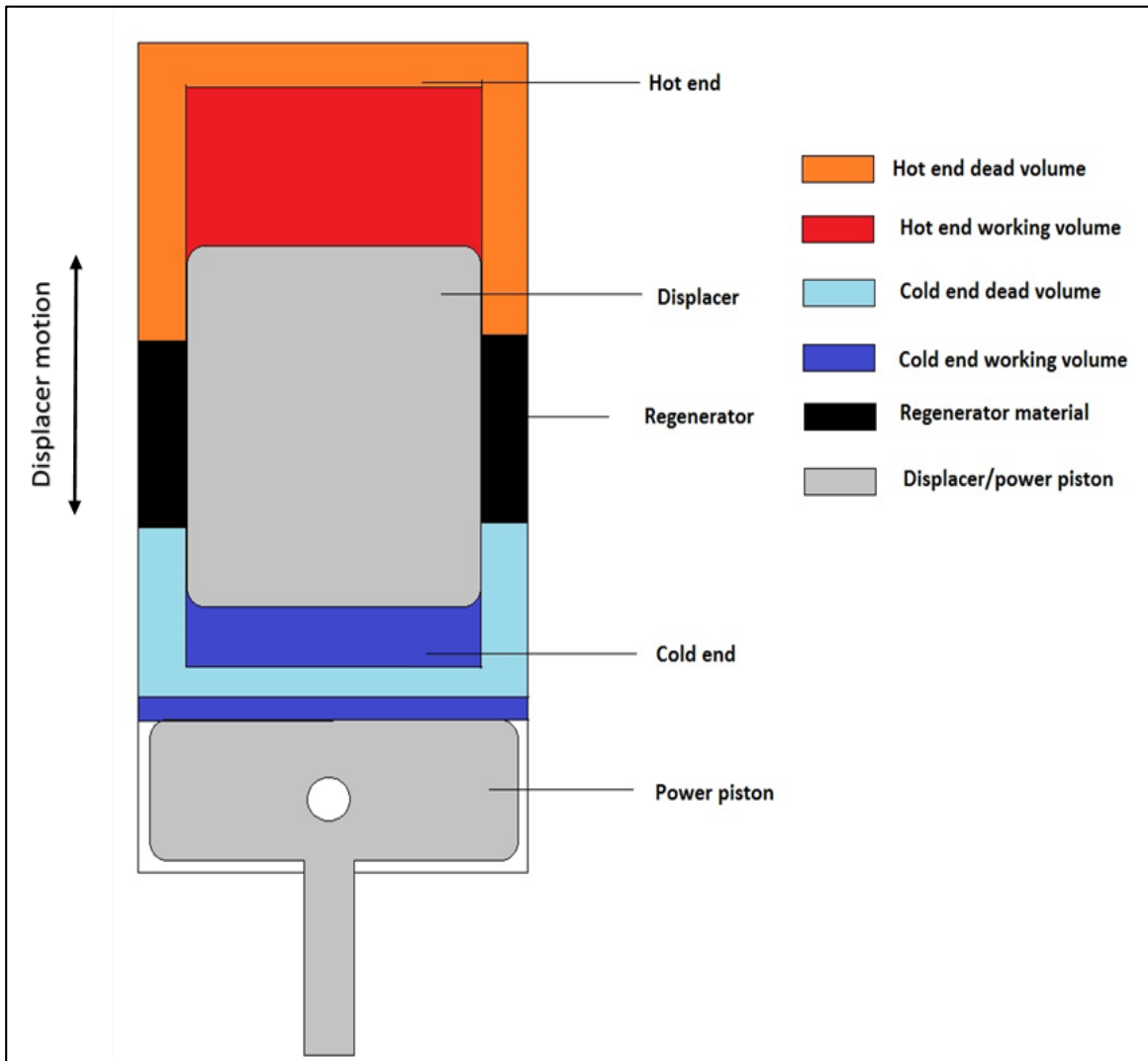


Figure 12: Control volume distribution for isothermal analysis

We now focus on free piston Stirling engine and its analysis. Before we proceed we divide the engine into different control volumes, on which we will be performing our analysis. At the hot end we have the hot end working

volume (in red) and the hot end dead volume (in orange). At the cold end we have the cold end working volume (deep blue) and the cold end dead volume (light blue). The cold end working volume is a sum of the swept volumes by the displacer as well as the power piston. Hence we have two separate volumes in deep blue which represent the working volume of the displacer and power piston. The isothermal analysis followed here is based on the analysis published in the Stirling engine design manual (11). Hence we define the nomenclature as used in the NASA design manual. For better understanding and quick reference, we will define the nomenclature here itself.

Nomenclature and symbols:

DB= displacer diameter, in cm

DC= diameter inside engine cylinder, in cm

HD= hot end dead volume, in cm^3

$3 \times RC$ = stroke of displacer, in cm

RD= regenerator volume (dead volume), in cm^3

CD= cold end dead volume, in cm^3

$2 \times R2$ = stroke of power piston, in cm

TH= effective gas temperature at hot end, in K

T_R = effective gas temperature in regenerator volume, in K

T_C = effective gas temperature at cold end, in K

M = total mass of working gas present in the engine, in gram mole

R = universal gas constant= 8.314 J/gmol-K

$P(N)$ = gas pressure inside cylinder at any point 'N' on the cycle, in MPa

Before the analysis is presented some important assumptions are to be made to simplify the analysis. These assumptions and their significance in our analysis are given in the following section.

Using isothermal analysis we will predict the instantaneous gas properties P , V , T and then calculate the work output from the cycle. But this analysis is simple because we will be dealing with only 1 unknown variable which is the pressure P . We will eliminate or constrain the other unknowns V and T to simplify our analysis. Note that T and V in real cycles do not behave as we will be assuming them to behave during isothermal analysis. The assumptions below will clarify things further.

Assumptions

- 1) The important assumption that is clear from the title of this analysis, 'isothermal' is that the temperature in the working volumes during the expansion and compression processes is assumed constant. This reduces the variable temperature to a constant value and reduces the number of unknowns in our analysis.
- 2) The volume in the engine is assumed to vary in a sinusoidal pattern. This is important to constrain the volume variable V . We can now evaluate the value of the volume V inside the engine at any given crank angle.
- 3) There is no gas leakage from the engine during operation. This is important because it implies that the total moles M of the gas inside the engine is constant. Thus using known T , V and M values we can calculate the pressure $P(N)$ at any instant N .
- 4) The working gas obeys ideal gas law. Obviously this has to be assumed if we are to calculate pressure using T , V and M values plugged into the ideal gas law.
- 5) The pressure is constant throughout the engine. This is important because we are calculating the PdV work at every instant and constant pressure is required to eliminate the VdP term.

- 6) Hot end and cold end engine temperatures are constant and equal to gas temperatures. Though this assumption does not affect the isothermal analysis but it is important. The assumption implies that the heat transfer to the working gas at hot and cold ends occurs without a temperature difference ΔT between the cylinder walls and working gas, and eliminates irreversibility accompanied by heat transfer across finite temperature difference.
- 7) The instantaneous work is given by PdV , instantaneous pressure times the change in instantaneous volume. The total work output from the cycle is given by the summation of all instantaneous work, summed over one entire cycle, that is, from crank angle of 0° to 360° .
- 8) Perfect regeneration takes place. This assumption is important because imperfection regeneration, which is encountered in real engines, drastically affects engine performance.
- 9) Frictional and other losses due to various heat transfer mechanisms are ignored.
- 10) The regenerator temperature is constant and equal to the logarithmic mean of the hot end and cold end temperatures.

Calculations for work and efficiency

We will perform the analysis in the following steps. These steps will also help in coding the analysis in Matlab.

- Assume known hot end and cold end temperatures.
- Select instantaneous crank angle increment in degrees.
- Calculate initial engine volume by assuming that crank angle is 0 when displacer is at topmost position.
- Assume that initial pressure is known, by measurement, and calculate moles M of gas present in engine. This value (M) will be constant throughout the cycle.
- Now calculate instantaneous volume inside engine for assumed instantaneous crank angle increment.
- Since T and M are constant, calculate new instantaneous pressure $P(N)$ for newly calculated instantaneous volume.
- Next calculate the differential work $dW = PdV$,
$$dV = V_{\text{new}} - V_{\text{previous}}$$
- Now repeat all above steps by incrementing crank angle for every iteration and take cumulative sum of work dW after every iteration.
- Once the crank angle reaches 360° , stop the iterations. We now have our work output W from the cycle in J/cycle.

The formulae to calculate the terms involved in above steps, are given as follows,

1) Regenerator temperature

$$TR = \frac{TH - TC}{\ln\left(\frac{TH}{TC}\right)}$$

2) Moles of working gas inside engine

$$M = \frac{P(1)(VA) \ln\left(\frac{TH}{TC}\right)}{R(TH - TC)}$$

3) Maximum hot end live volume

$$VL = \frac{\pi}{4}(2)(RC)(DB)^2$$

4) Maximum cold end live volume associated with displacer

$$VK = 2(RC)[(DB)^2 - (DD)^2]\left(\frac{\pi}{4}\right)$$

5) Maximum cold end volume associated with power piston

$$VP = 2(R2)[(DC)^2 - (DD)^2]\left(\frac{\pi}{4}\right)$$

6) Regenerator volume

$$RD = 2(LR)[(DB)^2 - (DD)^2]\left(\frac{\pi}{4}\right)$$

7) We now define 3 arrays to store 3 volumes, namely H(N) to store instantaneous hot end volume, C(N) to store instantaneous cold end volume and V(N) to store total instantaneous engine volume. The hot end live volume is given by

$$H(N) = \frac{VL}{2} [1 - \cos(F)] + HD$$

8) The cold end live volume at any instant N is given by

$$C(N) = \frac{VK}{2} [1 + \cos(F)] + CD + \frac{VP}{2} [1 - \cos(F - AL)]$$

9) The total volume at any instant N is then given by

$$V(N) = H(N) + C(N) + RD$$

10) Now the pressure at any instant can be given by

$$P(N) = \frac{(M)(R)}{\frac{H(N)}{TH} + \frac{C(N)}{TC} + \frac{RD}{TR}}$$

11) The change in volume will simply be

$$dV = V(N) - V(N - 1)$$

12) The instantaneous work will now be

$$dW(N) = P(N)dV$$

and total work will be

$$W(N) = W(N) + dW(N)$$

To get the work output per cycle we just repeat above calculations by differentially incrementing F from 0 to 360.

The following engine parameters are chosen to get the work output for the test case presented. These are not randomly chosen parameters, but have been decided after running the isothermal and adiabatic analysis numerous times and then optimizing them for the targeted power output.

Hot end working volume in $\text{cm}^3 = 134.7 \text{ cm}^3$

Cold end working volume in $\text{cm}^3 = 134.7 \text{ cm}^3$

Working piston working volume in $\text{cm}^3 = 84.823 \text{ cm}^3$

Hot end heat exchanger volume in $\text{cm}^3 = 30.9 \text{ cm}^3$

Cold end heat exchanger volume in $\text{cm}^3 = 30.9 \text{ cm}^3$

Regenerator volume in $\text{cm}^3 = 23.3165 \text{ cm}^3$

Hot end heat exchanger temperature in K = 800 K

Cold end heat exchanger temperature in K = 300 K

Effective regenerator temperature in K = 509.7727 K

Phase angle between displacer and working piston = 90°

Working gas is Helium

Mass of gas filled in engine = 0.1 moles

Specific heat ratio for Helium = 1.6667

The hot end heat exchanger and hot end working volume are constant and equal as we are assuming the process to be isothermal. Similarly the cold end heat exchanger and cold end working volume are assumed to be at the same constant temperature.

Output from code:

Work per cycle in J by numerical integration :

14.4500

The results of the isothermal analysis are compared with different formulae suggested by a number of published works. These formulae would be used for the same test case above.

The equation given by Mort Mayer, mentioned in the Stirling design manual [Martini, 4] is:

$$W_1 = \frac{M(R)(TC)(\pi)Y(VP)}{Y^2 + Z^2} \left(\frac{X}{(X^2 - Y^2 - Z^2)^{0.5}} - 1 \right)$$

where,

W_1 = work per cycle, J

M = gas inventory, g mol

R = gas constant = 8.314 J/g mol .K

T_C - effective cold gas temperature, K

T_H = effective hot gas temperature, K

T_C = effective cold gas temperature, K

$X = XX + (T_C/T_H) (XY)$

$XX = (V_P/2) + CD + (V_K/2) + (RD/2)$

$XY = HD + (V_L/2) + (RD/2)$

$Y = (V_L/2) (1 - T_C/T_H) \sin (AL)$

$Z = [V_P - V_L(1 - T_C/T_H) \cos(AL)]/2$

AL = phase angle between displacer and power piston

The work output from the code using this relation is:

Work per cycle in J by Mayers relation :

8.0687

The equation given by J.R.Senft, mentioned in the Stirling design manual [Martini, 4] is:

$$W1 = \frac{\pi(1 - AU)PX(VL)(XY)\sin(AL)}{Y + (Y^2 - X^2)^{0.5}} \left(\frac{Y - X}{Y + X}\right)^{0.5}$$

where,

$$X = [(AU - 1)^2 + 2(AU - 1)(XY)\cos(AL) + (XY)^2]^{0.5}$$

$$Y = AU + (4(XX)(AU)/(1 + AU)) + Z$$

$$Z = (1 + (XY)^2 - 2(XY)\cos(AL))^{0.5}$$

$$AU = TC/TH$$

$$XX = (RD + HD + CD)/VL$$

$$VL = VK$$

$$XY = VP/VL$$

The work output from the code using this relation is:

Work per cycle in J as per Senft equation :

15.8099

The equation given by Cooke-Yarborough for power output, mentioned in the Stirling design manual [Martini, 4] is:

$$W1 = \frac{\bar{P}(\pi) (VL)(VP)(TH - TC)\sin(AL)}{4 \left(XX \left(TC + \frac{XY}{XX}(TH - TC) \right) \right)}$$

where,

\bar{P} = mean pressure of working gas, which can be approximately calculated using following relation,

$$\bar{P} = \frac{(M)(R)}{\frac{(VL)}{2(TH)} + \frac{RD}{TR} + \frac{VK}{2(TC)} + \frac{VP}{2(TC)}}$$

The work output from the code using this relation is:

Work per cycle in J by Cooke-Yarborough relation :

16.7089

All above relations are obtained by simplifying the Schimdt theory. A detailed study about the Schimdt theory can be found in the work by Hirata (13).

Adiabatic analysis of the Stirling cycle

Introduction

Till now, it was assumed that the expansion and compression processes in the engine occur isothermally. The actual expansion and compression process is far from isothermal. If we assume the expansion and compression process to be adiabatic it makes the analysis more realistic

as compared to the isothermal analysis. The isothermal analysis helps in preliminary analysis only. The further analysis is to be made complicated to get better and more realistic results. For the purpose of this analysis we divide our engine into 5 control volumes, and assume that the expansion and compression processes follow the adiabatic law

$$PV^\gamma = \text{constant}$$

Where,

γ = ratio of specific heat of working fluid = 1.67 for He

Assumptions

Almost all the assumptions are similar to that of the isothermal analysis with the following additional assumptions,

- a) The expansion and compression process is adiabatic
- b) The temperature of hot end heat exchanger, cold end heat exchanger and regenerator is constant.
- c) The working fluid obeys ideal gas law.
- d) The specific heats for the working fluid are constant. (Since Helium is the working gas, the specific heats are constant for Helium, so this is actually true and not an assumption).
- e) The pressure is uniform throughout the engine at all instants.

- f) The volume inside the engine varies in a sinusoidal manner.
- g) There is no leakage of working fluid from the engine.
- h) Perfect regeneration occurs in the regenerator volume.
- i) The heat transfer in the hot end heat exchanger and cold end heat exchanger occurs at constant temperature.
- j) The initial pressure is known.
- k) 0° crank angle corresponds to topmost position of displacer.

Description

The figure below explains the different sections of the engine that will be analyzed. Note that in adiabatic analysis we are assigning a dead volume to the working volume, unlike the isothermal analysis, in which the working volumes has zero dead volumes associated with them. The hot and cold end working are assumed to be perfectly insulated and follow adiabatic compression and expansion processes respectively. This is an attempt to move away from the ideal isothermal processes towards a more realistic process. In reality the expansion and compression processes are not adiabatic, nevertheless assuming them to be adiabatic gives better results that are more useful.

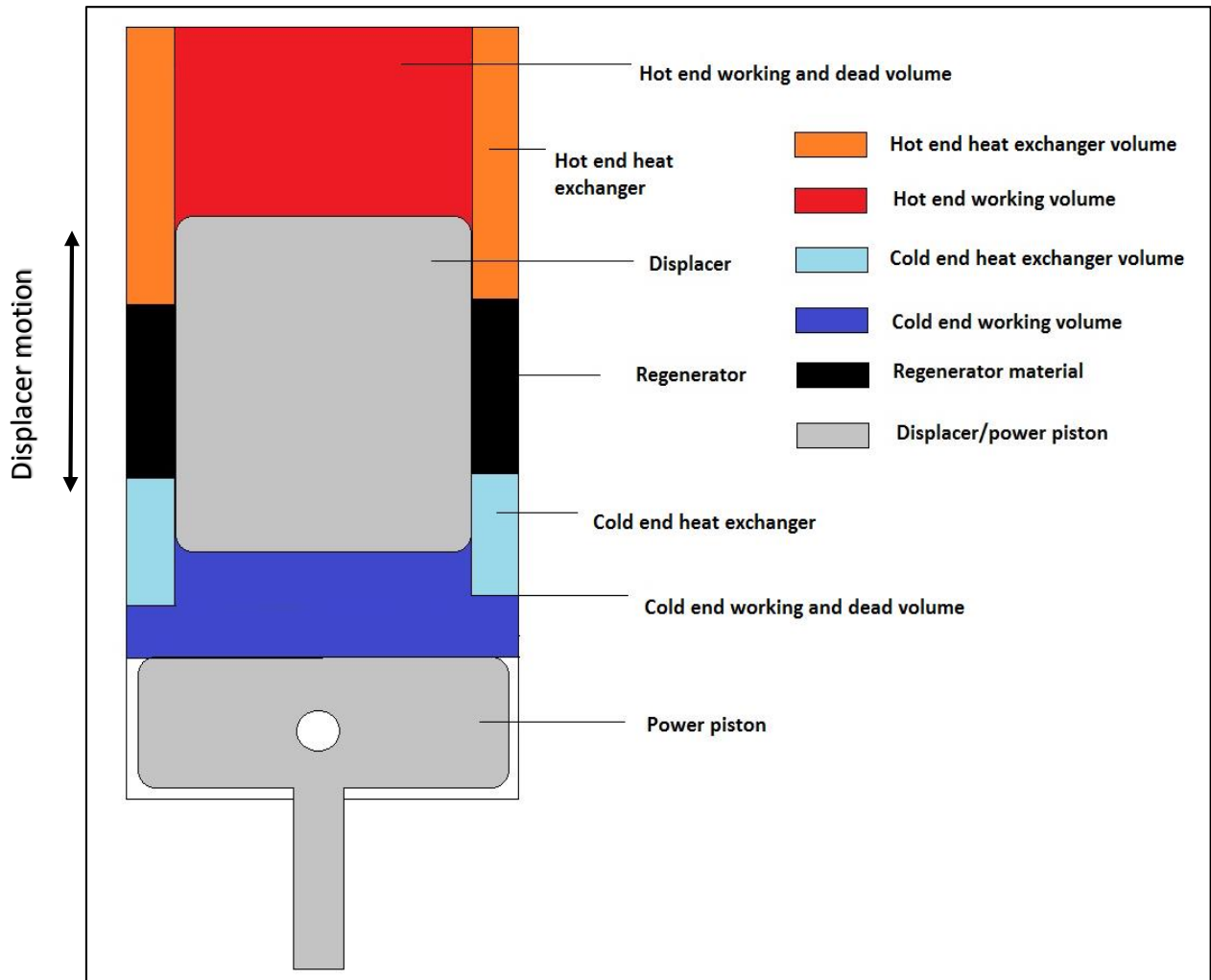


Figure 13: Control volume distribution for adiabatic analysis

As seen in the above figure, for the purpose of analysis, the engine is divided into 5 volumes as shown. The energy balance equation will be applied to every control volume. In this case again the instantaneous volume is known, as sinusoidal volume variation is assumed. And the total moles of gas is also constant because there is no leakage. So there are two variables, pressure in the engine and temperature in the expansion and

compression spaces. The temperatures in the hot end heat exchanger, cold end heat exchanger and the regenerator are constant. The temperature in the expansion and compression spaces can be predicted as they follow the adiabatic expansion/compression law. Hence we can write the temperature in terms of pressure variable and then use conservation of mass to get an implicit equation for the unknown pressure. Now there are two methods to get a solution to the obtained implicit equation of pressure,

Method 1: Direct approximate analytical solution given by Urieli and Berchowitz, and presented in the thesis work by Jose Martinez, (12).

Method 2: Use iterative method with initial guess for pressure. Here give an initial guess for the unknown pressure p and calculate the error in mass balance. Then extrapolate the guess close to the solution using the error values obtained. This method is described in the Stirling engine design manual [Martini, 4]. Instead of iterating the p value the solve function available in Matlab can be used to get the solution. However this function is time consuming and increases run time for the code.

For the present analysis method 1 shall be used, which gives an approximate analytical solution. The exact solution can be obtained by performing a few iterations. The detailed approach will be described in the following sections. Now for the purpose of applying energy balance to our control volumes, define our nomenclature for the analysis. Since this

analysis is complicated and every data point should be recorded for the purpose of better understanding, the nomenclature will be extensive and include two dimensional arrays.

Nomenclature and symbols:

$2 \times R_2$ = stroke of power piston, in cm

$3 \times R_C$ = stroke of displacer, in cm

AL=phase lag

DB= displacer diameter, in cm

DC= diameter inside engine cylinder, in cm

Dp= change in pressure, in MPa

f=crank angle

g_{Ack} =mass flow from compression space to cold end heat exchanger space

g_{Ahe} = mass flow from hot end heat exchanger space to expansion space

g_{Akr} = mass flow from cold end heat exchanger to regenerator space

g_{Arh} = mass flow from regenerator space to hot end heat exchanger space

h= clearance between cylinder top/bottom and displacer top/bottom when displacer is at topmost/bottommost position respectively.

LC= cold end heat exchanger length

LH= hot end heat exchanger length

M= total mass of working gas present in the engine, in gram mole

mc=compression space mass

me=expansion space mass

mec=cold end heat exchanger mass

meh=hot end heat exchanger mass

mr=regenerator mass

p=instantaneous pressure

R= universal gas constant= 8.314 J/gmol-K

r= C_p/C_v for the working gas

Tc=compression space temperature

Tce=cold end heat exchanger temperature

Te=expansion space temperature

The=hot end heat exchanger temperature

Tr=regenerator temperature

Vc=Cold end volume

Vcd=cold end dead volume

V_{ce} =cold end heat exchanger volume

V_d =cold end maximum displacer volume

V_e =Maximum Hot end volume

V_{hd} =hot end dead volume

V_{he} =Hot end heat exchanger volume

V_p =cold end maximum piston volume

V_r =regenerator volume

DV_c = change in volume in compression space

DV_e = change in volume in expansion space

Dm_c = change in mass in compression space

Dm_e = change in mass in expansion space

Dm_{ce} = change in mass in cold end heat exchanger space

Dm_{he} = change in mass in hot end heat exchanger space

Dm_r = change in mass in regenerator space

T_{ck} , T_{he} = conditional temperatures varying as per instantaneous mass flow direction

Energy balance and other equations

Energy balance on the engine is done by applying the first law to every section of the engine and then solving the simultaneous differential equations to get a solution for pressure, temperature and mass variations inside the engine during a cycle. To model the system perform energy balance on each of the five volumes inside the engine. The energy balance for all the volumes is shown in the box diagram below. The big box represents the engine, which is the larger control volume. The smaller boxes represent the individual volumes inside the engine. These five boxes are the individual control volumes. Both heat and mass flow across these individual smaller control volumes, while only heat can flow across the outer, bigger control volume representing the engine. The individual energy balance for each control volume is written and then solved for the mass and temperature variables. The analysis involves a complex differential equations. The solution for pressure and other variables is taken from the work by Martinez (12) as well as Urieli and Berchowitz (14) in their respective works.

Firstly the energy balance between two control volumes is shown for simplicity. After that energy balance for the entire engine shall be shown in a single figure.

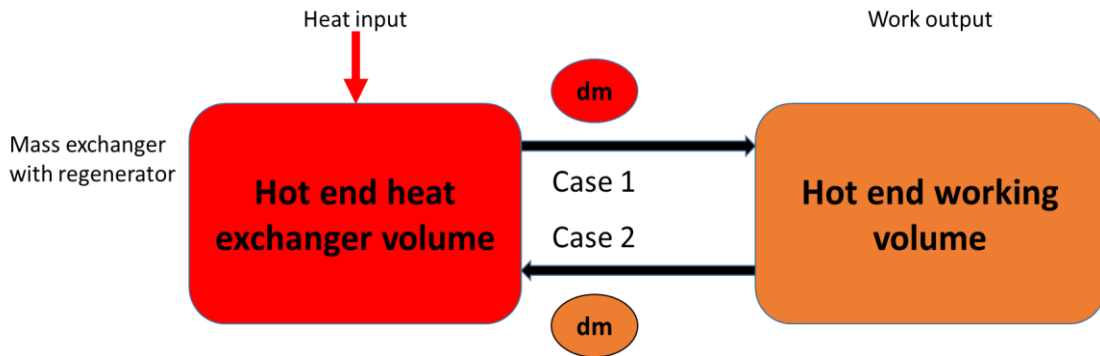


Figure 14: Energy balance for hot end volumes only

Two cases are possible for mass (and hence energy) exchange between the two volumes at hot end.

Case 1: The gas flows from the hot end heat exchanger to the hot end working volume at the hot end heat exchanger temperature.

Case 2: The gas flows from the hot end working volume to the hot end heat exchanger at the hot end working volume temperature.

The thing to be noted is that the work flowing in or out of the working volume has not been shown in the figure. The mass exchange of the hot end heat exchanger has also been ignored in the figure. This mass exchange will have two similar cases. However both work and mass exchange with regenerator shall appear in the energy balance equation. At any given instant there is no uniform direction of mass flow in the engine. It will depend solely on the thermodynamic property changes of each control volume. It is important to determine mass flow direction at each instant to perform energy balance.

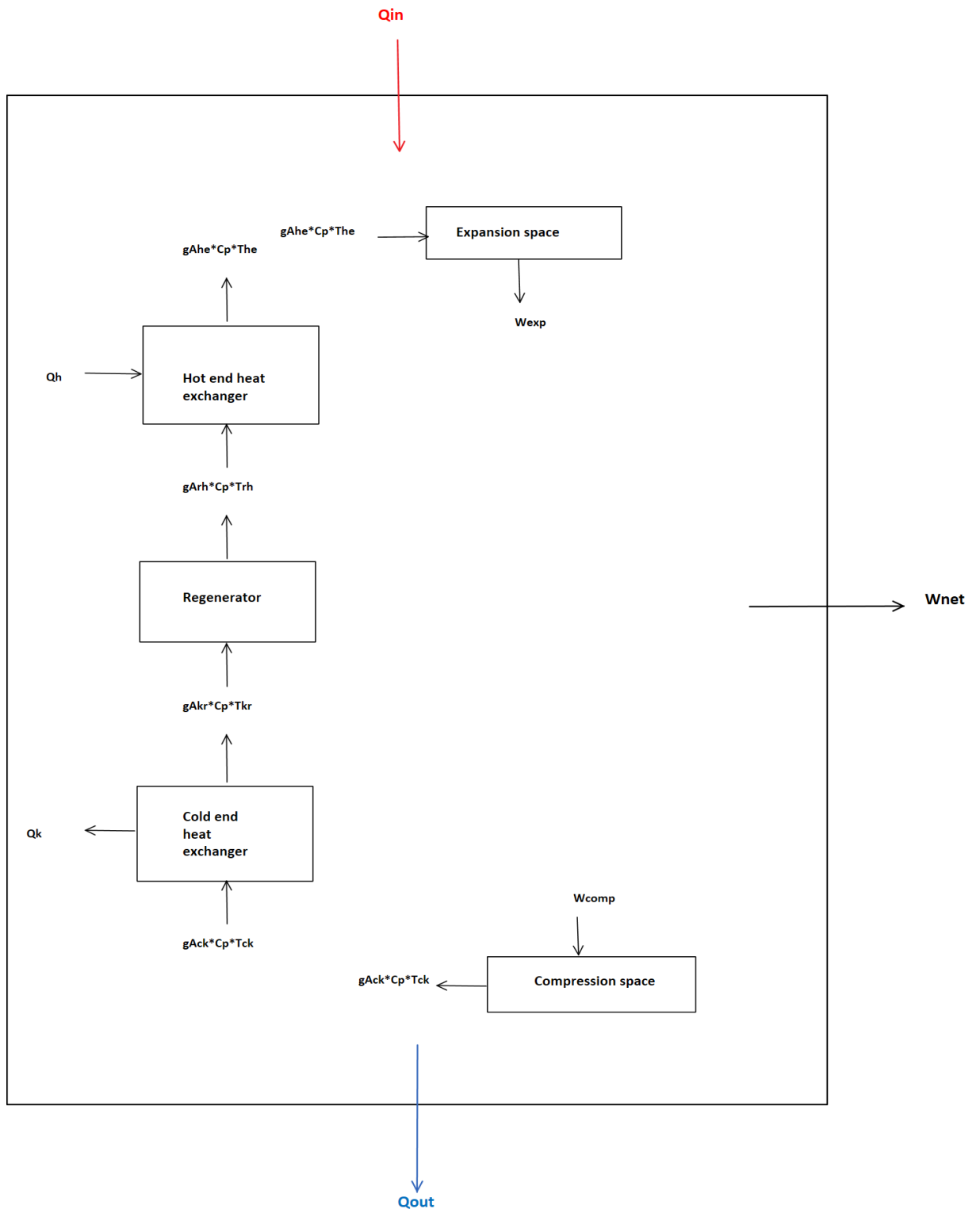


Figure 15: Energy balance for the control volumes

The above figure explains the energy balance applied on all the control volumes. The $g_{Ack} \cdot C_p \cdot T_{ck}$ and other similar terms is nothing but the heat energy given by the equation $m \cdot C_p \cdot dT$. The other things to be noted are that pressure losses in the individual control volumes are ignored and heat transfer in the heat exchanger is assumed at constant temperature. Using the above energy balance the work and efficiency is calculated. The flowchart for the analysis is presented below.

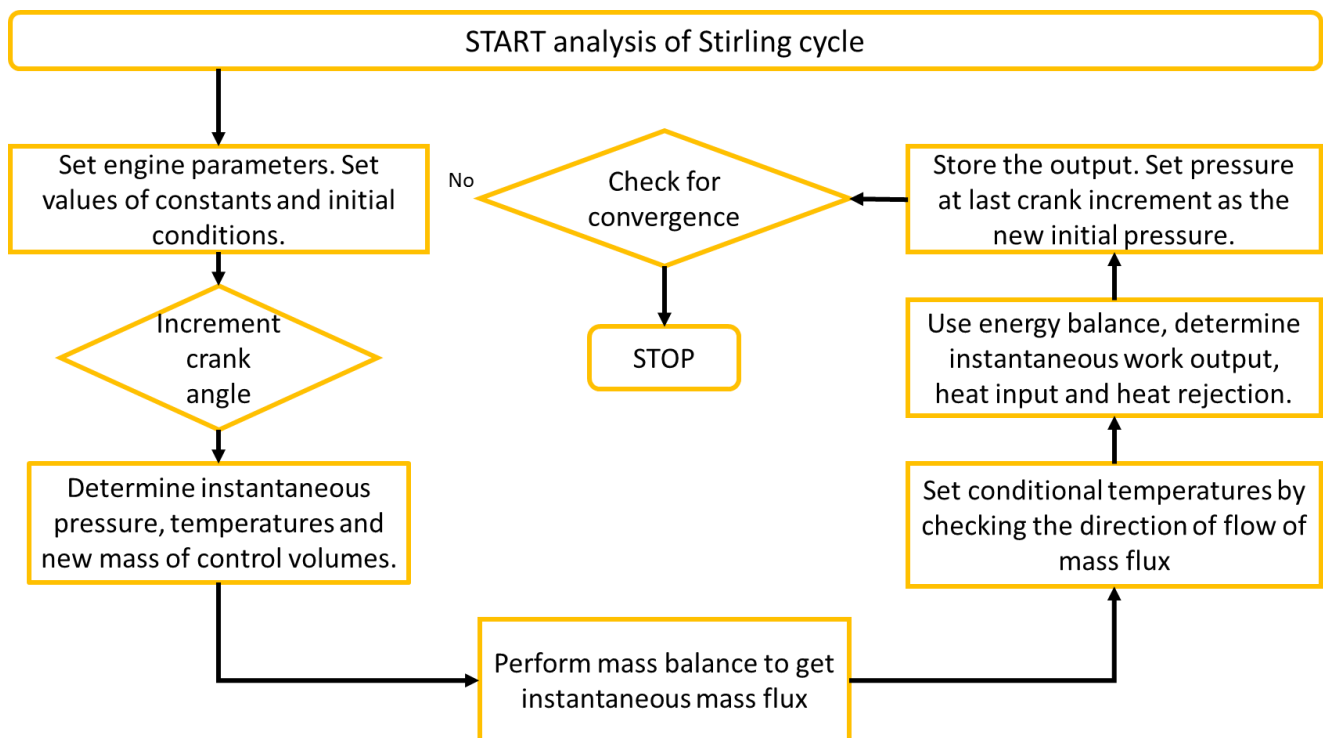


Figure 16: Flowchart for second order analysis

Approach to programming the analysis

The modeling would be done using mass and energy balance on individual control volumes. Using the mass and energy balance relations, instantaneous pressure, temperatures and work or heat exchange with the surroundings will be calculated. The procedure will be iterated for one complete cycle and the cumulative values of power, heat exchanged and efficiency are found at the end of the cycle. The different parameters will be calculated sequentially in the Matlab code based on the following formulae-

- 1) Regenerator temperature (assumed constant throughout cycle)

$$Tr = \frac{T_H - T_C}{\ln\left(\frac{T_H}{T_C}\right)}$$

- 2) Moles of working gas inside engine (constant throughout cycle)

$$M = \frac{P(1)(VA) \ln\left(\frac{T_H}{T_C}\right)}{R(T_H - T_C)}$$

- 3) Maximum hot end live volume (constant)

$$V_{em} = \frac{\pi}{4}(2)(RC)(DB)^2 \text{ or calculated value for specific engine design}$$

- 4) The hot end dead volume is given by (constant)

$$V_{ed} = 2(h)[(DB)^2 - (DD)^2]\left(\frac{\pi}{4}\right) \text{ or calculated value for specific engine design}$$

5) The instantaneous hot end live volume is given by

$$V_e = \frac{V_{em}}{2}[1 - \cos(F)] + V_{ed} \text{ or calculated value for specific engine design}$$

6) Maximum cold end live volume associated with displacer

$$V_{cm} = 2(RC)[(DB)^2 - (DD)^2]\left(\frac{\pi}{4}\right) \text{ or calculated value for specific engine design}$$

7) The cold end dead volume is given by

$$V_{cd} = 2(h)[(DB)^2 - (DD)^2]\left(\frac{\pi}{4}\right) \text{ or calculated value for specific engine design}$$

8) The cold end live volume at any instant N is given by

$$V_c = \frac{V_{cm}}{2}[1 + \cos(F)] + V_{cd} + \frac{V_p}{2}[1 - \cos(F - AL)]$$

9) Regenerator volume

$$V_r = 2(LR)[(DB)^2 - (DD)^2]\left(\frac{\pi}{4}\right) \text{ or calculated value for specific engine design}$$

10) The hot end heat exchanger volume is given by

$$V_{he} = 2(LH)[(DB)^2 - (DD)^2]\left(\frac{\pi}{4}\right) \text{ or calculated value for specific engine}$$

design

11) The cold end heat exchanger volume at any instant is given by

$$V_{ce} = 2(LC)[(DB)^2 - (DD)^2]\left(\frac{\pi}{4}\right) \text{ or calculated value for specific engine design}$$

- 12) The total volume at any instant N is then given by

$$V(N) = V_c + V_{cd} + V_e + V_{ed} + V_{he} + V_{ce} + V_r$$

- 13) The analytical formula for change in pressure based on energy balance is

$$Dp = - \frac{\gamma p \left(\left(\frac{DV_c}{T_{ck}} \right) + \left(\frac{DV_e}{T_{he}} \right) \right)}{\left(\frac{V_c}{T_{ck}} \right) + \gamma \left(\frac{V_{ce}}{T_{ce}} + \frac{V_r}{T_r} + \frac{V_{he}}{T_{he}} \right) + \frac{V_e}{T_{he}}}$$

- 14) The change in mass in compression space is given as

$$Dm_c = \frac{pDV_c + \frac{V_c Dp}{\gamma}}{\frac{R}{T_{ck}}}$$

- 15) The mass content in the cold end heat exchanger, regenerator, hot end heat exchanger and expansion spaces is respectively given as

$$m_{ce} = \frac{(p)(V_{ce})}{(R)(T_k)}$$

$$m_r = \frac{(p)(V_r)}{(R)(T_r)}$$

$$m_{he} = \frac{pV_{he}}{RT_{he}}$$

$$m_e = M - (m_c + m_{ce} + m_r + m_{he})$$

- 16) The temperatures in the expansion and compression spaces are then given by

$$T_e = \frac{(p)(V_e)}{(R)(m_e)}$$

$$T_c = \frac{(p)(V_c)}{(R)(m_c)}$$

- 17) The change in mass in the cold end heat exchanger, regenerator and hot end heat exchanger is given by

$$Dm_{ce} = \frac{(m_{ce})(Dp)}{p}$$

$$Dm_r = \frac{(m_r)(Dp)}{p}$$

$$Dm_{he} = \frac{(m_{he})(Dp)}{p}$$

- 18) The mass exchanges between the control volumes are given by

$$g_{Ack} = -Dm_c$$

$$g_{Akr} = g_{Ack} - Dm_{ce}$$

$$g_{Arh} = g_{Akr} - Dm_r$$

$$g_{Ahe} = g_{Arh} - Dm_{he}$$

19) Now the conditional temperatures T_{ck} and T_{he} are assigned values as below. Note that before the first iteration, T_{ck} and T_{he} may be assigned the values T_c and T_h respectively

$$\text{If } g_{Ack} > 0 \quad \text{then, } T_{ck} = T_c \quad \text{else, } T_{ck} = T_k$$

$$\text{If } g_{Ahe} > 0 \quad \text{then, } T_{he} = T_h \quad \text{else, } T_{he} = T_e$$

20) Finally the differential work, heat input at hot end heat exchanger, regenerator heat and heat given out at cold end heat exchanger are given respectively as

$$DW = p(DV_c + DV_e)$$

$$DQ_k = \frac{(V_{ce})(Dp)(C_v)}{R} - C_p((T_{ck})(g_{Ack}) - (T_{kr})(g_{Akr}))$$

$$DQ_r = \frac{(V_r)(Dp)(C_v)}{R} - C_p((T_{kr})(g_{Akr}) - (T_{rh})(g_{Arh}))$$

$$DQ_h = \frac{(V_{he})(Dp)(C_v)}{R} - C_p((T_{kr})(g_{Akr}) - (T_{he})(g_{Ahe}))$$

The differential work and heat transfers are added cumulatively to get the total work and heat exchanges of the engine per cycle. The entire process is to be again repeated until a stable solution is obtained, that is, the variation in pressure over the entire cycle stabilizes.

Chapter 4 – GPU-3 engine analysis and code validation

The GPU-3 Stirling engine was developed by General Motors. It is a beta configuration Stirling and one of the Stirling engines to be commercialized. Extensive experimental performance analysis of the GPU-3 Stirling has been documented by NASA in the handbook authored by Martini (11). These published results would be used to draw a comparison between the engine performance predicted by the developed code and the actual performance. To start with, it is important to understand the construction of the GPU-3 Stirling and its key design parameters that include working volumes, operating temperatures and mean pressure.

The program for adiabatic analysis of the GPU-3 is provided in the Appendix section of this report. For the purpose of validation, the GPU-3 Stirling engine parameters are introduced in the code and the results and characteristics are studied against those published by NASA and other sources. The GPU-3 is one of the most successful Stirling engines built by General Motors. It has an array of published works which are available quite easily. This makes the engine more suitable for comparison and validation. The GPU-3 can operate at different mean engine pressure and different heater temperatures. Extensive studies at different working pressures and temperatures has been published by NASA in the Stirling

engine design manual (11). A schematic of the GPU-3 engine is shown below. It is a beta configuration with rhombic drive.

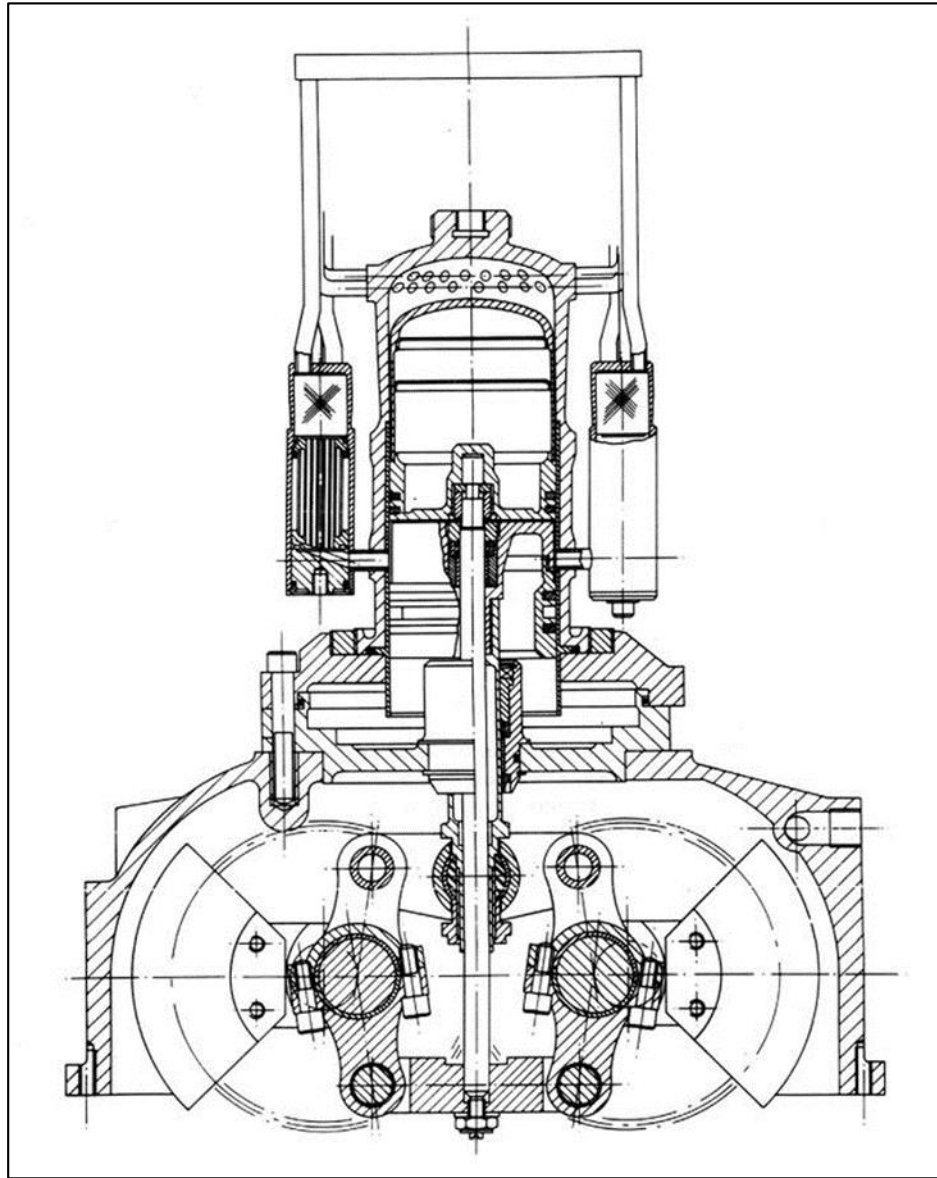


Figure 17: Construction of GPU-3 engine

The specifications for the GPU-3 Stirling engine are shown in below figure.

Parameters	Values
Clearance volumes	
Compression space	28.68cm ³
Expansion space	30.52cm ³
Working gas	Helium
Swept Volumes	
Compression space	113.14cm ³
Expansion space	120.82cm ³
Regenerator void volume	50.55cm ³
Hot end heat exchanger volume	70.88cm ³
Cold end heat exchanger volume	13.8cm ³

Figure 18: Specifications for GPU-3 engine

These specifications are sufficient to perform a detailed thermodynamic analysis of the engine. The results from the code and the actual performance results have been plotted in the same graph to facilitate comparison between the two. The power output is the key comparison parameter for the engine. The combined thermodynamic and dynamical code power output is recorded and the mechanical loss value (provided by NASA) is subtracted. This final power output value is then compared with the actual power output value. The corresponding heater and cooler temperatures used can be found on each graph. The mean operating pressure is also shown on each graph. The initial pressure guess needs to be adjusted in the code until the code predicts a mean pressure output equal to that in the published result test case.

A few plots have been shown below, before the performance analysis graphs, to study and understand the working of the GPU-3. These include the volume

variation during the cycle, the pressure variation over a cycle, P-V diagram for GPU-3, hot and cold end temperature variation over a cycle, mass flow and mass content variation over a cycle and finally the instantaneous work variation. These plots help in understanding exactly what goes on inside the engine and how an effective positive work output is obtained through one cycle.

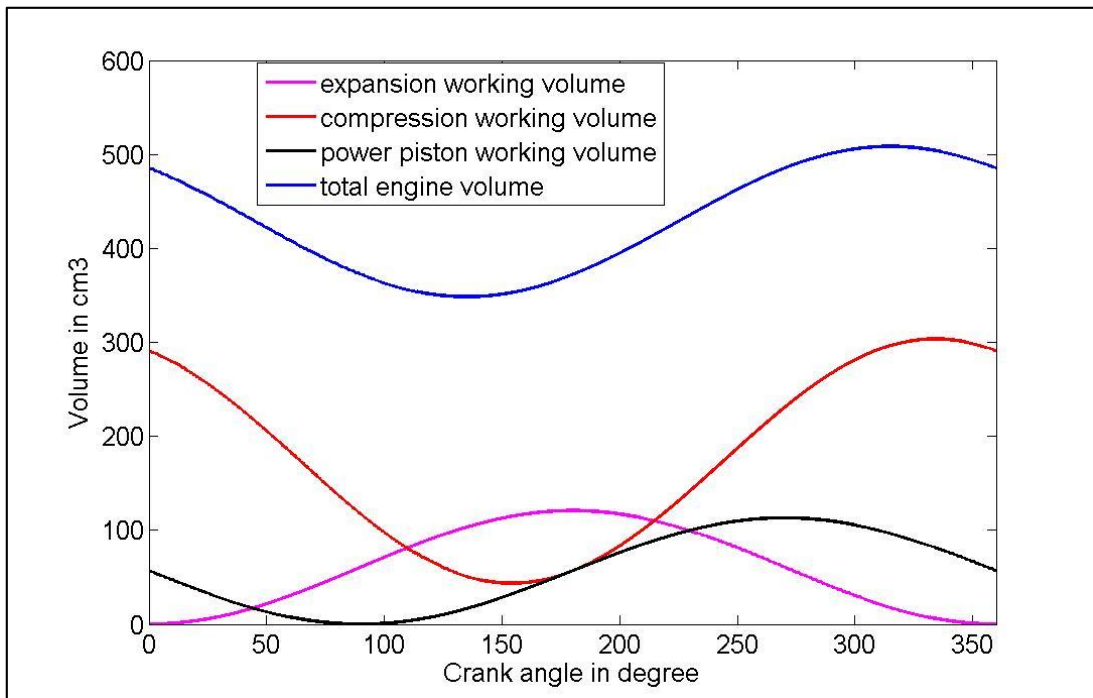


Figure 19: Volume variation during cycle

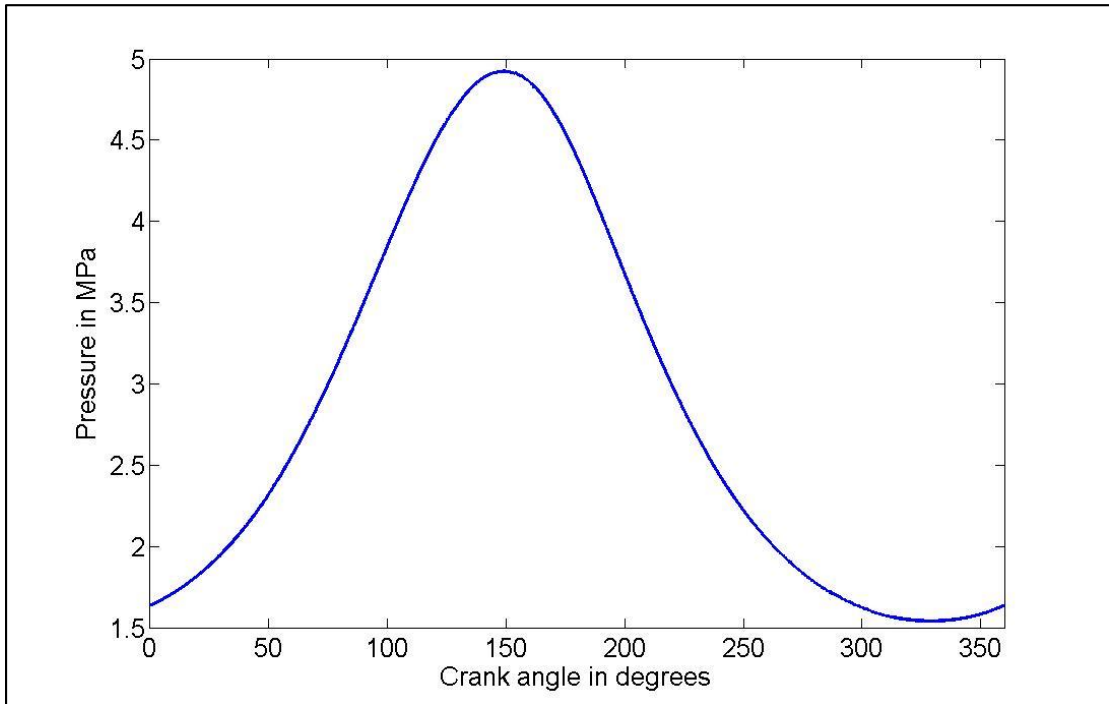


Figure 20: Pressure variation during cycle

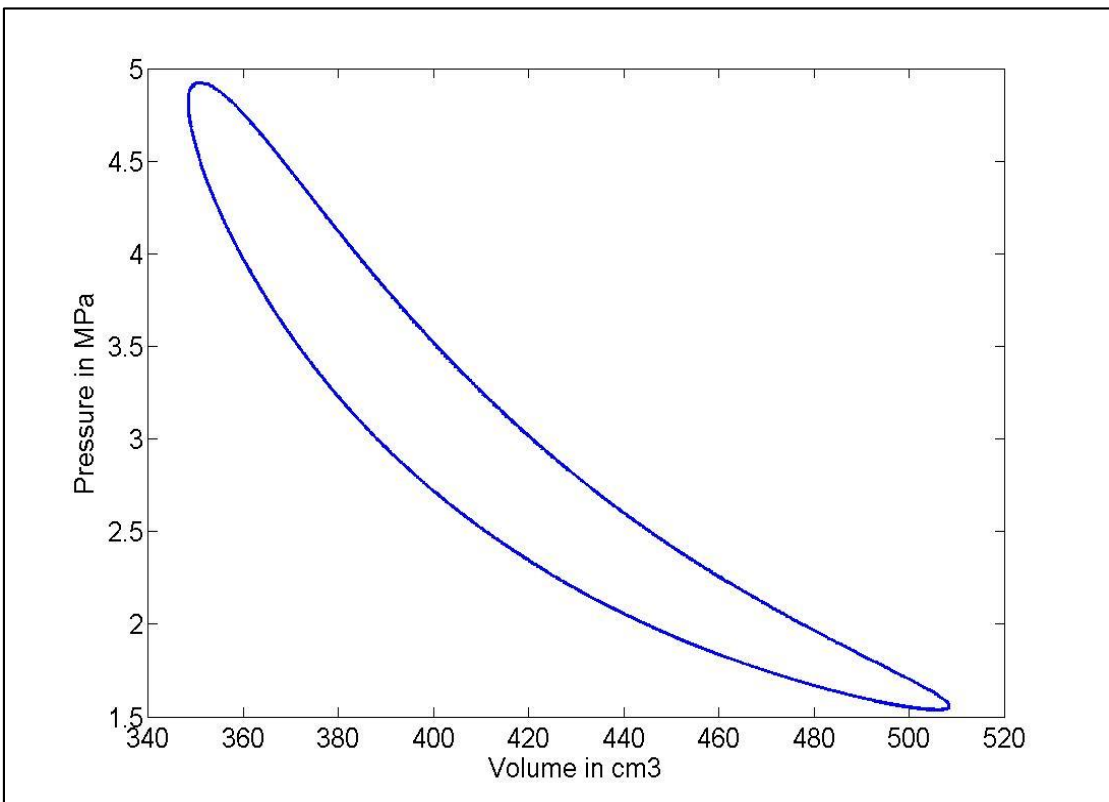


Figure 21: PV diagram for the GPU-3 engine

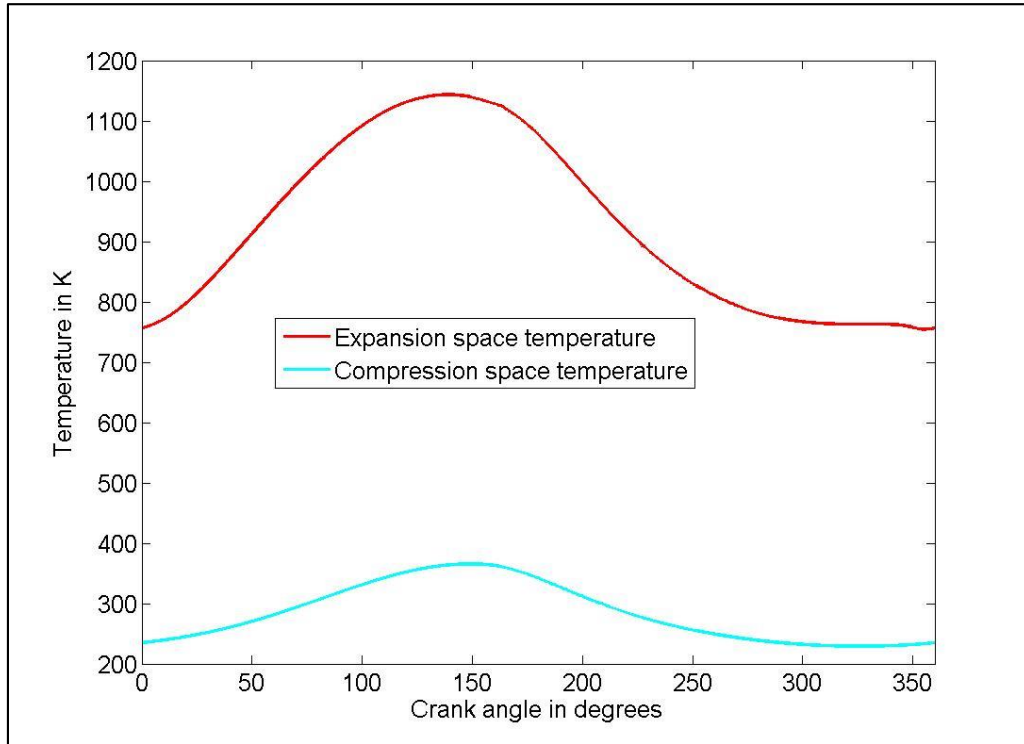


Figure 22: Temperature variation for GPU-3 during cycle

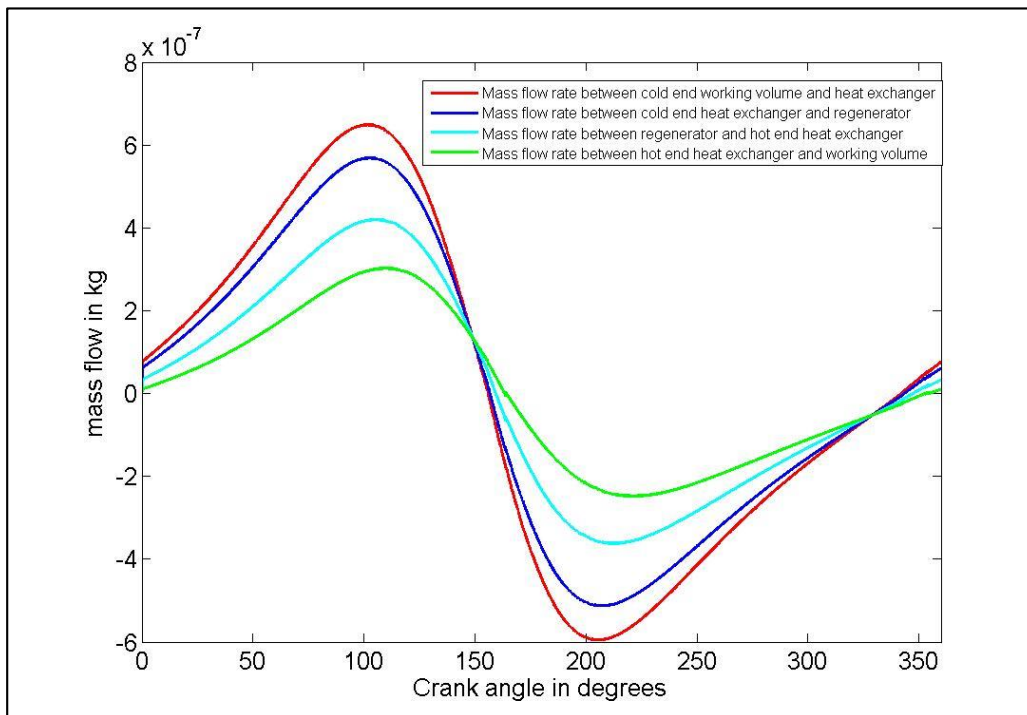


Figure 23: Mass flow in control volumes for GPU-3 during cycle

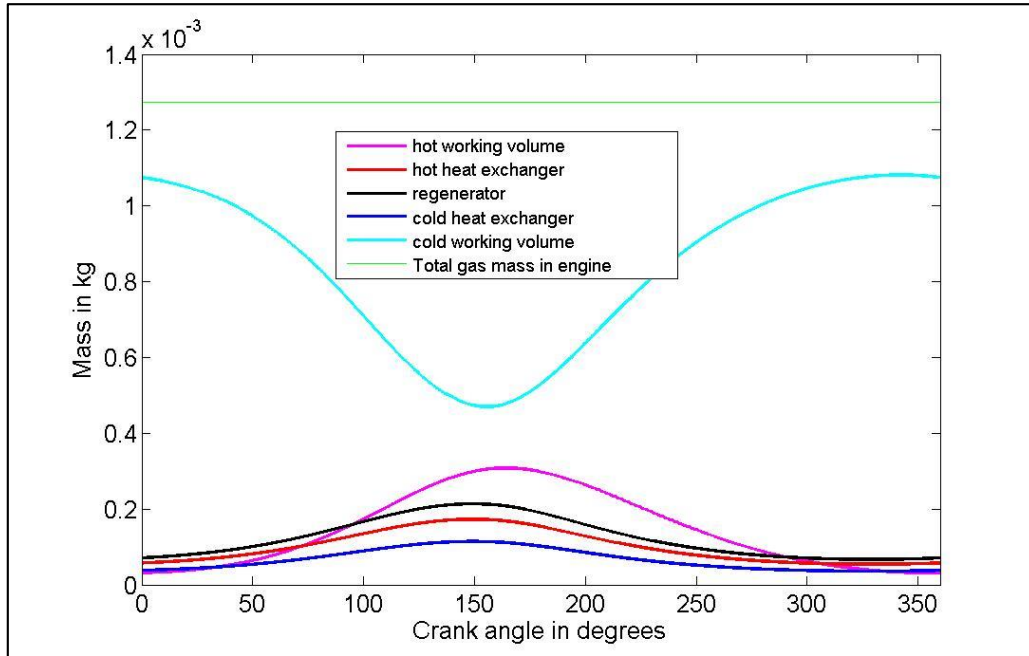


Figure 24: Mass variation in control volumes for GPU-3 during cycle

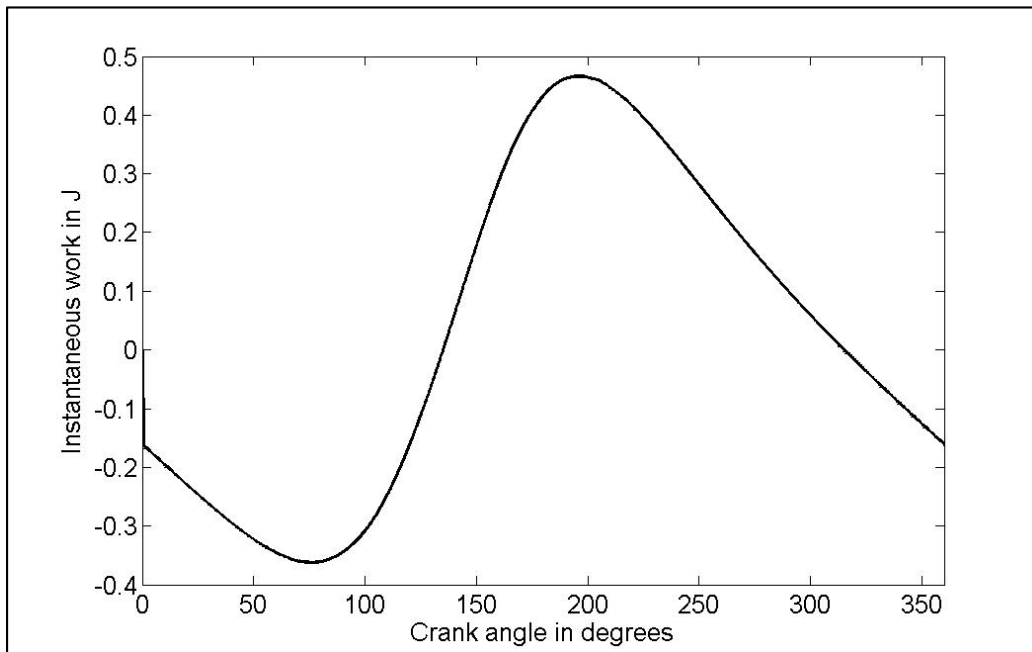


Figure 25: Instantaneous work for GPU-3 during cycle

Comparison of GPU-3 results from code with published work

Initially a comparison of the thermodynamic analysis alone is made with the actual results. The result of this comparison will also establish the necessity of a dynamical analysis. The following graph shows a comparison between power outputs for the GPU-3 at a mean operating pressure of 2.76MPa, heater temperature of 868K and cooler temperature of 288K.

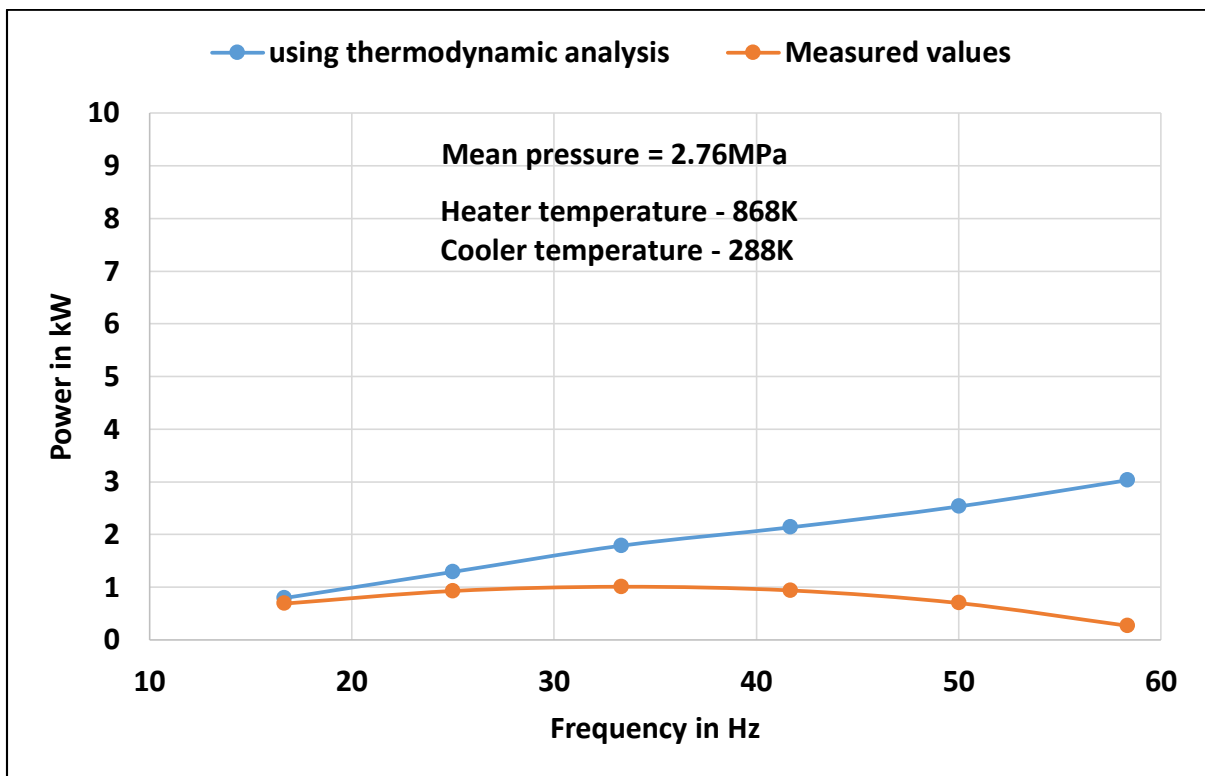


Figure 26: Power output comparison at 2.76MPa

It can be observed that as the operating frequency increases the deviation of analytical results from actual increases significantly. This is because the thermodynamic analysis alone does not consider the effects of operating

frequency and losses associated with operating frequency. The viscous a losses are proportional to the operating frequency and significant at high operating frequencies. At lower frequencies the thermodynamic analysis alone is sufficient and fairly accurate. Next the power outputs are compared at the same operating mean pressure of 2.76MPa but at a higher heater temperature of 922K.

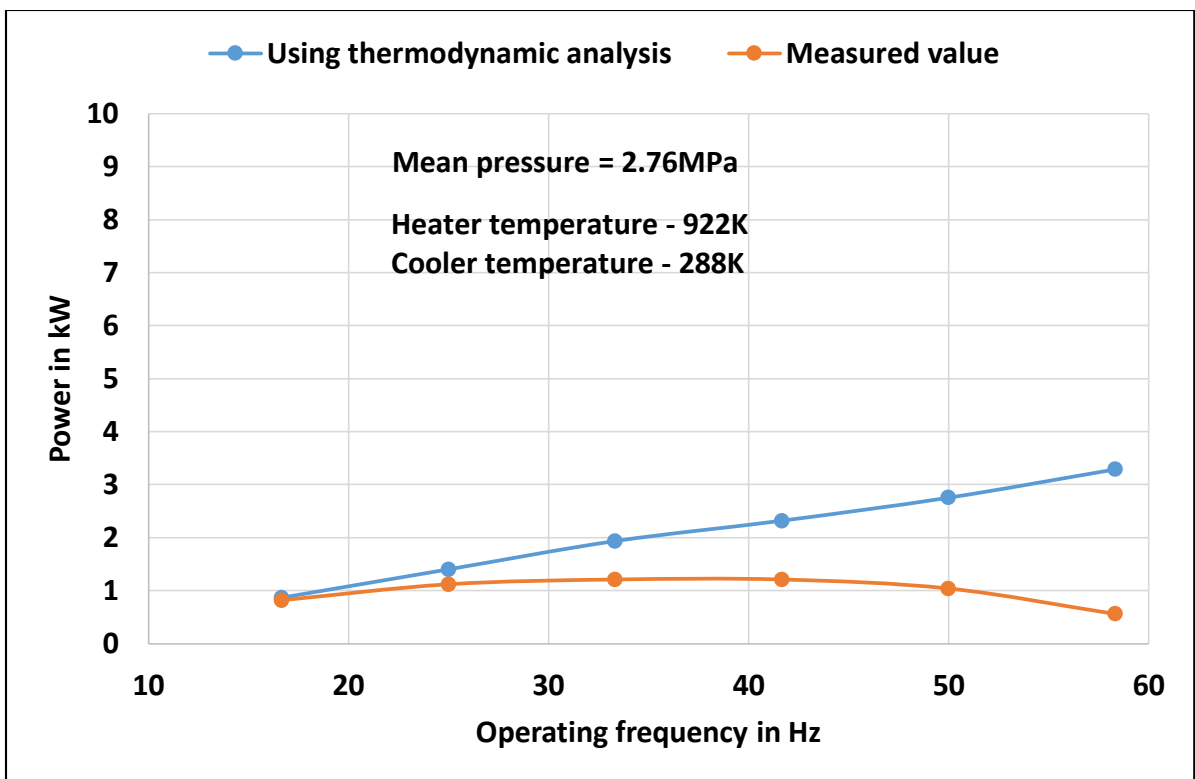


Figure 27: Power output comparison at 2.76MPa

The nature of the comparison remains almost same except that the accuracy of the thermodynamic analysis is higher at lower operating frequencies. Since the heater temperature is higher, the mean cycle temperature also rises

resulting in higher efficiency, thus tending towards analytically predicted output. This comparison shows that as operating temperature increases at lower frequencies the thermodynamic analysis alone becomes more accurate. According to the Beale power equation, the power output is linearly proportional to mean operating pressure. But practically power output does not increase linearly with mean operating pressure due to higher fluid friction and leakage losses at higher pressure. Thus the thermodynamic analysis alone is expected to deviate more from actual performance at higher mean operating pressures.

The following graph gives a comparison between power output predicted by the thermodynamic analysis alone and the actual power output with a mean operating pressure of 5.52MPa, heater temperature of 868K and cooler temperature of 288K. A significant deviation from actual results is observed even at lower operating frequencies. This is because even at lower frequencies viscous and leakage losses are higher on account of higher operating mean pressure. At higher operating frequencies, this deviation amplifies further, strongly suggesting the need for an analysis that will consider viscous losses and damping. These parameters are accounted for in the dynamical losses and the noticeable difference in performance output prediction will be presented subsequently.

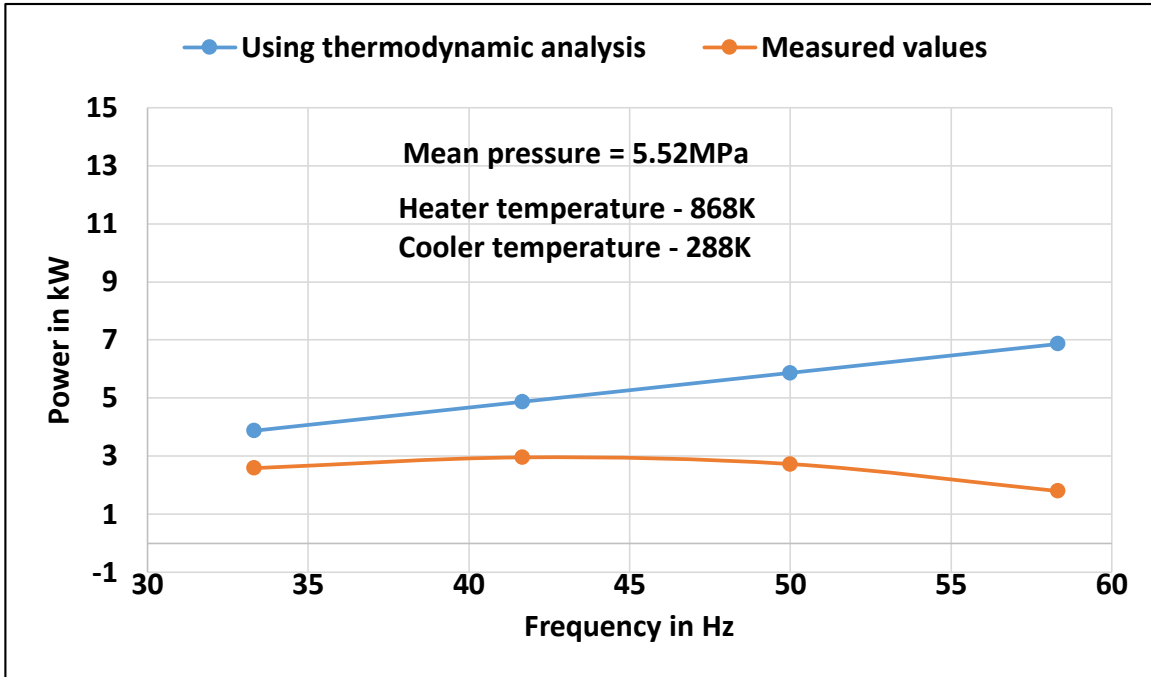


Figure 28: Power output comparison at 5.52MPa

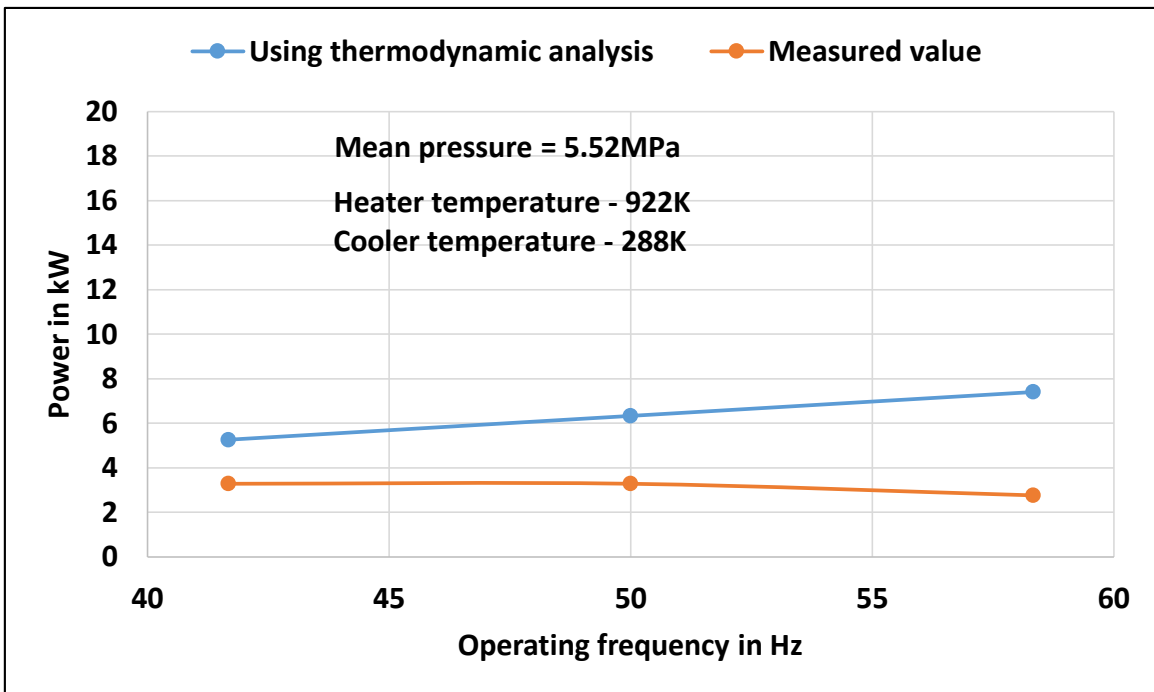


Figure 29: Power output comparison at 5.52MPa

Next, in Fig 31 a comparison for the power is presented for the same operating pressure of 5.52MPa but at a higher heater temperature. The results published by NASA have been reproduced below from (11). The same points have been plotted in graphs shown above.

Pt	Mean Press		Engine Speed		Brake Power	
	MPa	PSIa	HZ	RPM	KW	HP
1	2.76	400	16.67	1000	0.69	0.93
2	2.76	400	25	1500	0.93	1.25
3	2.76	400	33.33	2000	1.01	1.35
4	2.76	400	41.67	2500	0.94	1.26
5	2.76	400	50	3000	0.70	0.94
6	2.76	400	58.33	3500	0.27	0.36
7	5.52	800	33.33	2000	2.59	3.47
8	5.52	800	41.67	2500	2.96	3.97
9	5.52	800	50	3000	2.73	3.66
10	5.52	800	58.33	3500	1.80	2.42

Figure 30: Power output published by NASA

The above table shows power output values for a heater temperature of 922K. It is important to remember that the working gas used is Helium and both, the analysis and the published results, are strictly for Helium gas. If an analysis for hydrogen gas or other working fluid is to be done then necessary changes in constant should be done in the Matlab code.

Now after the necessity for the dynamical analysis has been established, the results for the combined thermodynamic and dynamical analysis have been presented in following sections.

First a general comparison between the power outputs predicted by the combined analysis and the actual power output, for varying mean operating pressure. The results have been tabulated in below figure. The highlighted columns give the power outputs for the code and actual measured respectively.

Sr. No	Mean pressure	Frequency	Analysis output	Heat transfer losses	Indicated power by analysis	Mechanical loss	Brake power by analysis results	Measured brake power	Input power by analysis	Input power	Brake efficiency by analysis	Measured efficiency
	MPa	Hz	kW	kW	kW	kW	kW	kW	kW	kW	%	%
1	2.76	33.33	2.75	0.63	2.12	0.8	1.32	1.21	5.4	6.64	24.59	18.22
2	4.14	41.67	5.13	0.78	4.35	1.4	2.94	2.42	10.15	11.33	29.02	21.3
3	5.52	50	7.23	0.94	6.29	1.9	4.39	3.28	15.59	17.45	28.19	22.5

Figure 31: Power output using combined analysis

The table has power output for the GPU-3 at three operating pressures. The operating frequencies corresponding to these pressures are the optimum frequencies for that particular pressure. The analysis output is the power output obtained from the code. The heat transfer loss value for the specific operating conditions has been provided in the work by Timoumi (15). The mechanical loss values have been published by NASA and the mechanical losses graph has been reproduced below.

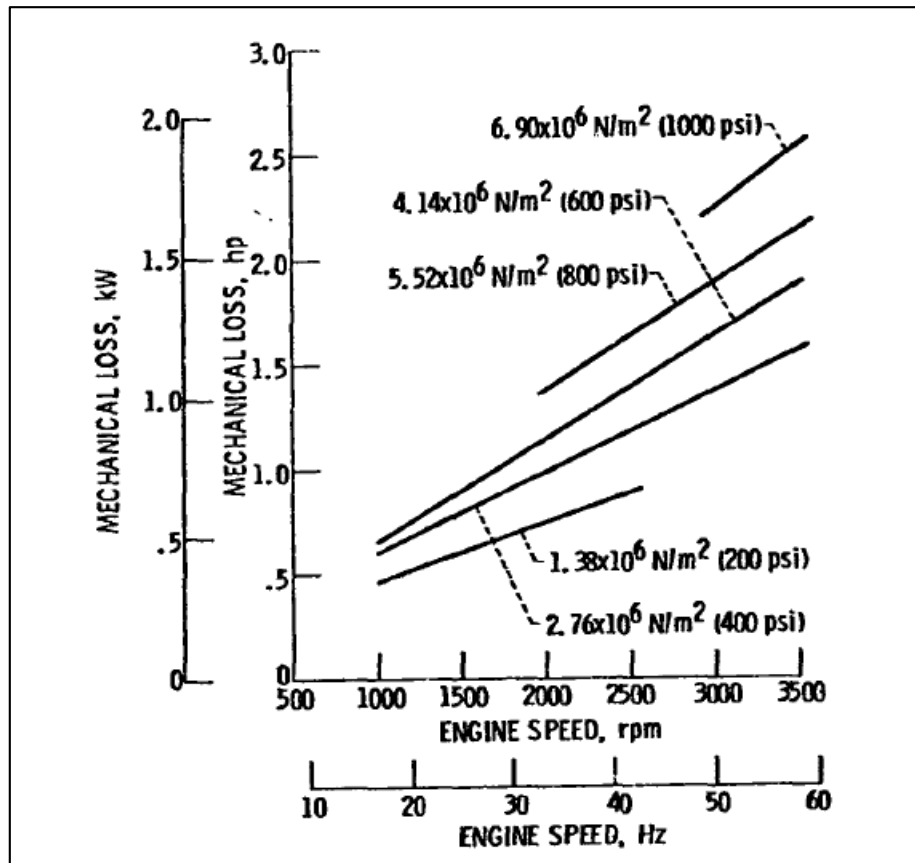


Figure 32: Mechanical loss value for GPU-3

For ease of comparison the tabulated data is plotted in the graph that follows. The black curve shows the power output predicted by the combined analysis. The red line is the predicted power output after subtracting heat transfer losses and mechanical losses. Finally the purple line is the actual measured power output. The analytical results consider viscous damping losses, heat transfer losses and mechanical losses. However the gas leakage due to imperfect sealing and heat transfer losses are not considered. The deviation in predicted and actual results is on account of these losses and a few other minor energy losses.

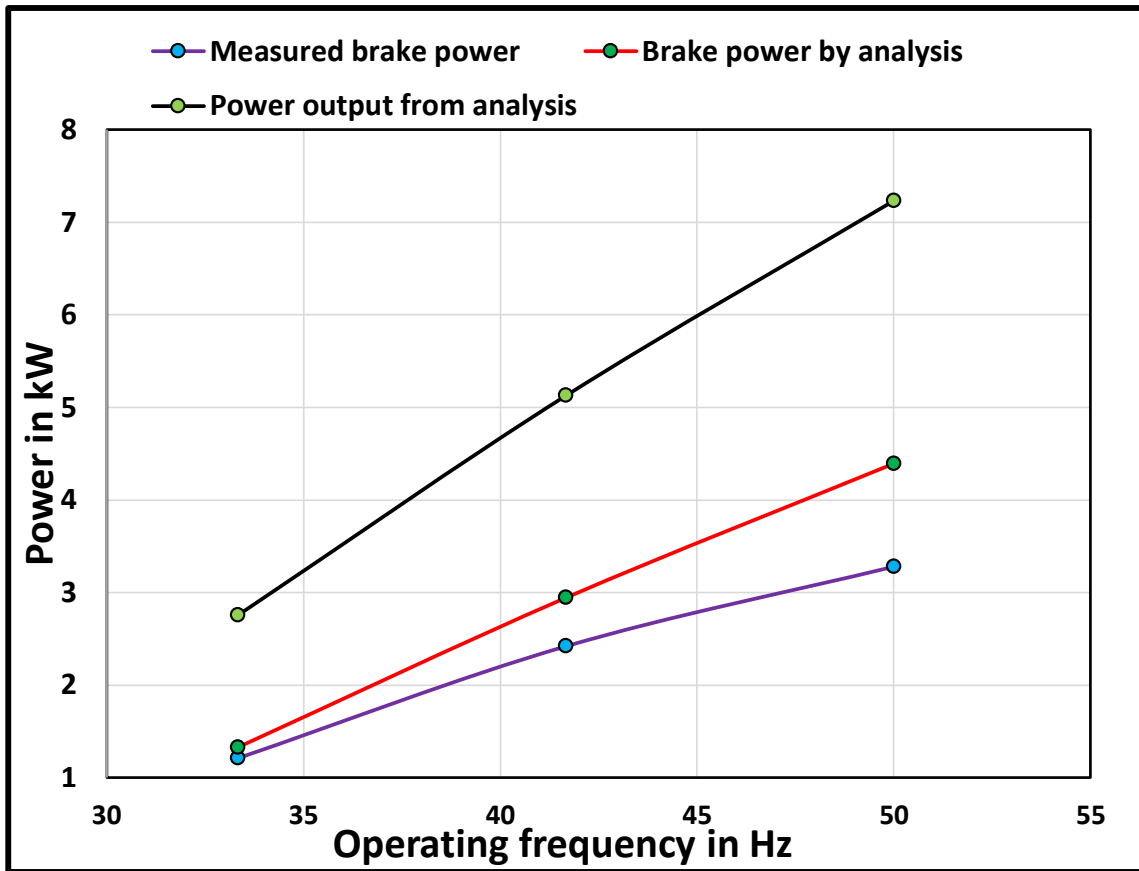


Figure 33: Power output comparison for combined analysis

The next graph shows the comparison between the heat input to the heater per cycle. The analytical results predict a lower heat input requirement than the actual required. There are two reasons for this. Firstly, the clearance dead volume of the GPU-3 engine has been assigned to the working space volumes. Usually these are considered a part of the heat exchanger volumes. Secondly, the engine is assumed to be perfectly insulated with no internal or external conductive, convective or radiative heat loss. This results in lower heat input requirement for the same power output.

In the graph below, the black curve represents the analytical heat input requirement to the hot end heat exchanger and the purple curve represents the actual measured heat input to the hot end heat exchanger or heater. The deviation remains consistent throughout irrespective of the operating frequency because the operating frequency does not significantly affect heat loss to external surroundings.

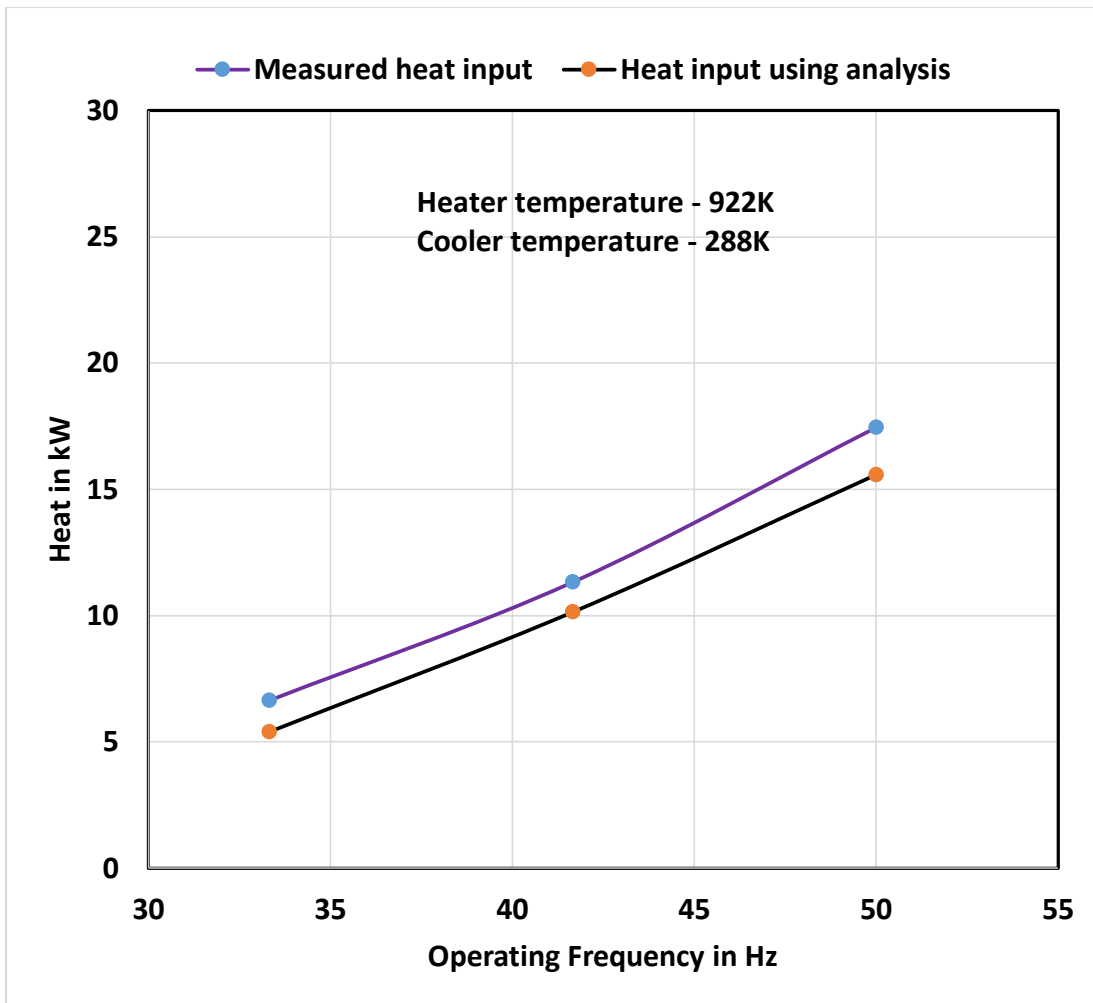


Figure 34: Heat input to GPU-3 engine

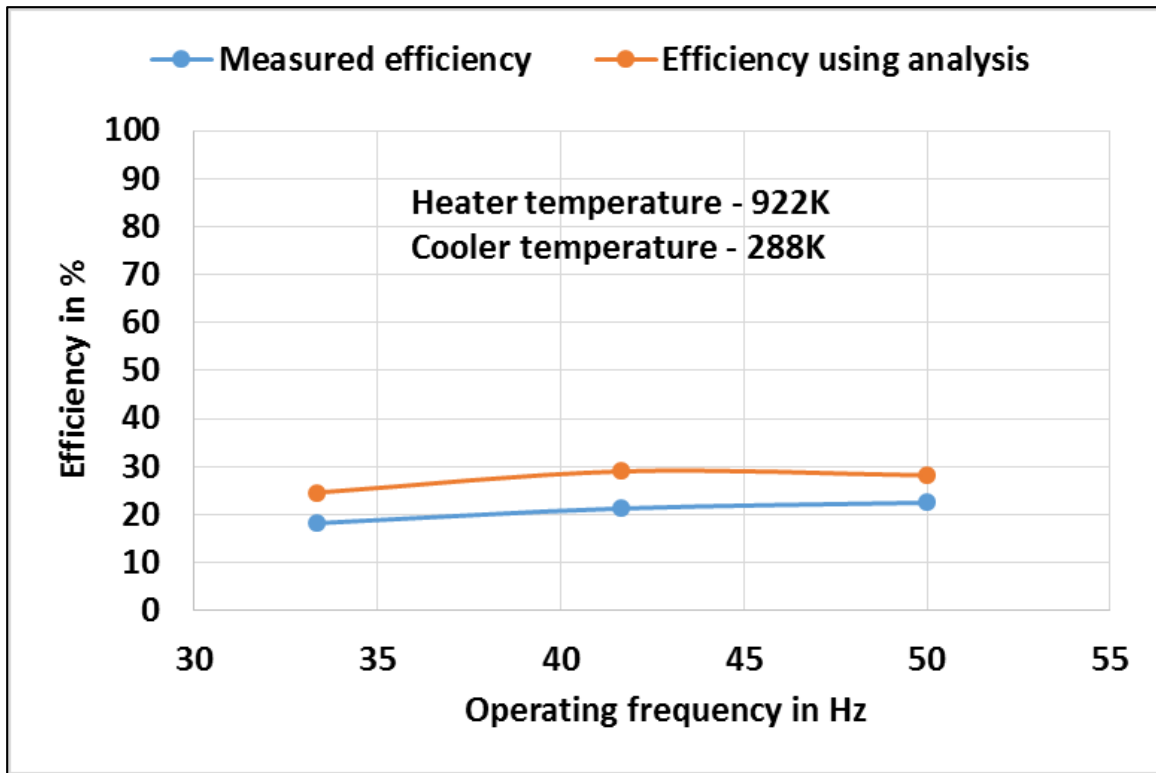


Figure 35: Efficiency comparison for GPU-3

Figure 27 shows a comparison between efficiency of the GPU-3 engine by combined analysis and actual measured value. The analysis predicts a higher efficiency which is expected since it predicts higher power output at lower heat input to the heater. However the deviation is not much and fairly accurately predicts the engine efficiency, when compared to other second order analysis methods used for the GPU-3 engine. A smaller step size and consideration of the clearance volume as a part of working volume allows for better and more accurate results when combined with an extensive dynamical analysis model.

Many previous analysis methods ignore the clearance dead volumes in their calculations. The below figure shows the significance of the clearance dead volume with respect to accuracy of the analysis. Certainly, considering the clearance dead volume will give better and accurate results at the cost of added complexity in the analysis. Using thermodynamic analysis alone, the blue line shows the power output without clearance volume consideration and the orange line shows the predicted power output with consideration of clearance volume. The black line is the actual measured power output.

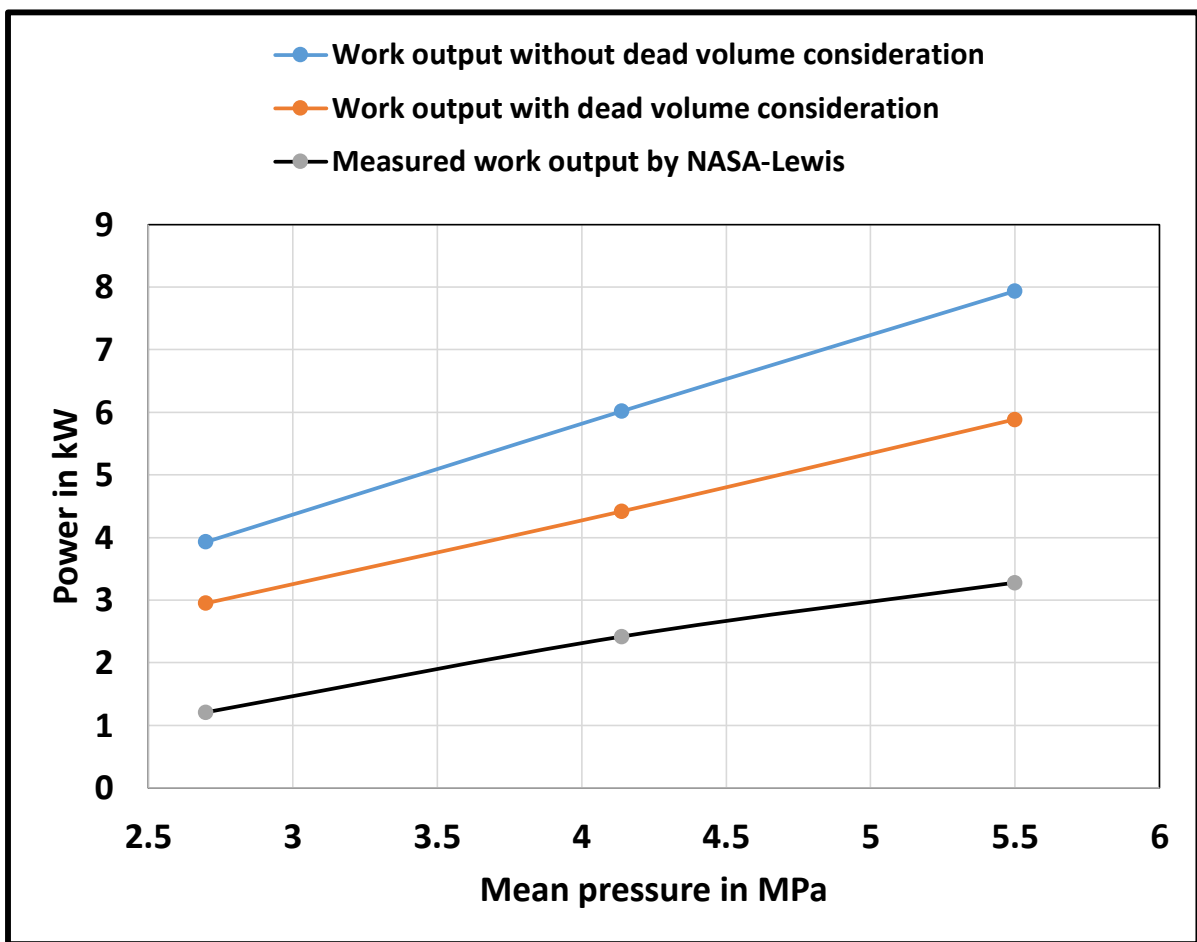


Figure 36: Effect of clearance volume

Compression ratio optimization of the GPU-3 Stirling engine.

A thermodynamically optimized compression ratio can be found for the GPU-3 by varying the distribution of working volumes among the displacer and power piston, while keeping the total working volume constant. The working volumes are looped in the code. Each volume distribution will have a different compression ratio. The power output and efficiency against the compression ratio have shown below in their respective plots. It is noteworthy that there are different compression ratios for optimum efficiency and optimum power output. That is the maximum efficiency does not correspond with the maximum power output and vice versa. Thus a compromise of the two needs to be selected. According to the analysis, the maximum efficiency should be obtained at a compression ratio of about 1.34. The maximum power output should be obtained at a compression ratio of 1.4. The actual compression ratio used in the GPU-3 is 1.43 which indicates that it is designed for giving maximum power output. The efficiency values indicated are the adiabatic efficiencies where the operating frequency is assumed to be constant. Of course these efficiencies will be lower when the dynamical analysis is also taken into account. But at a given constant operating frequency, the nature of the efficiency and power output curve shall remain the same. There is also an optimum operating frequency corresponding to every operating pressure which can be observed in the results published by NASA.

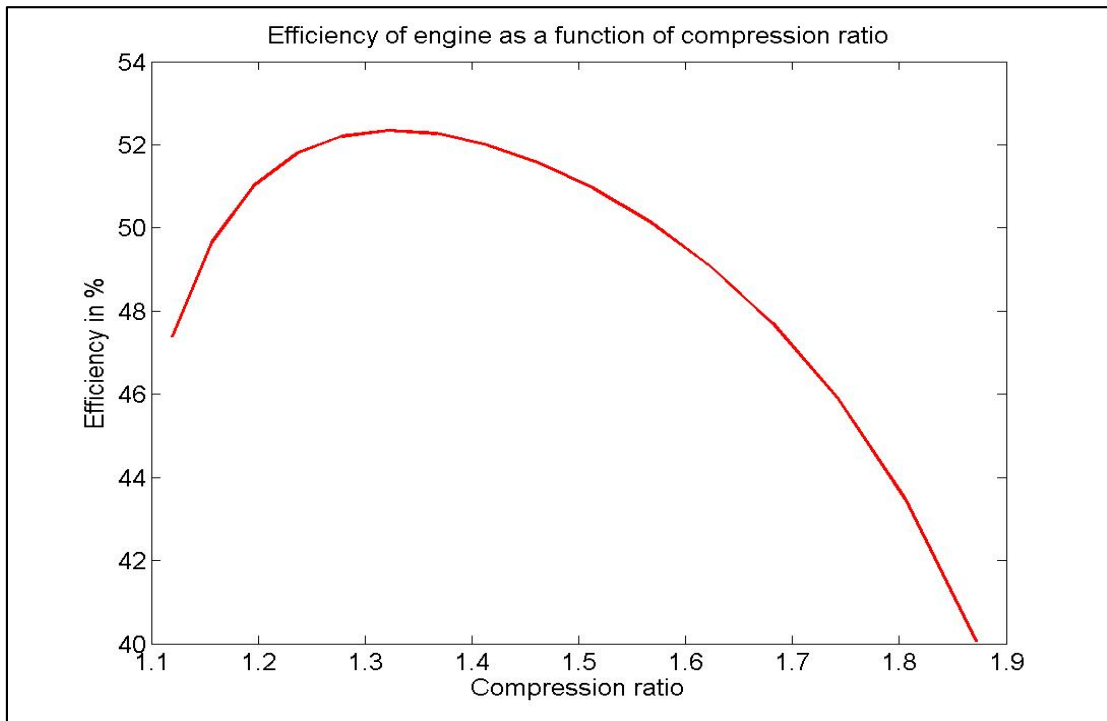


Figure 37: Compression ratio optimization for maximum efficiency

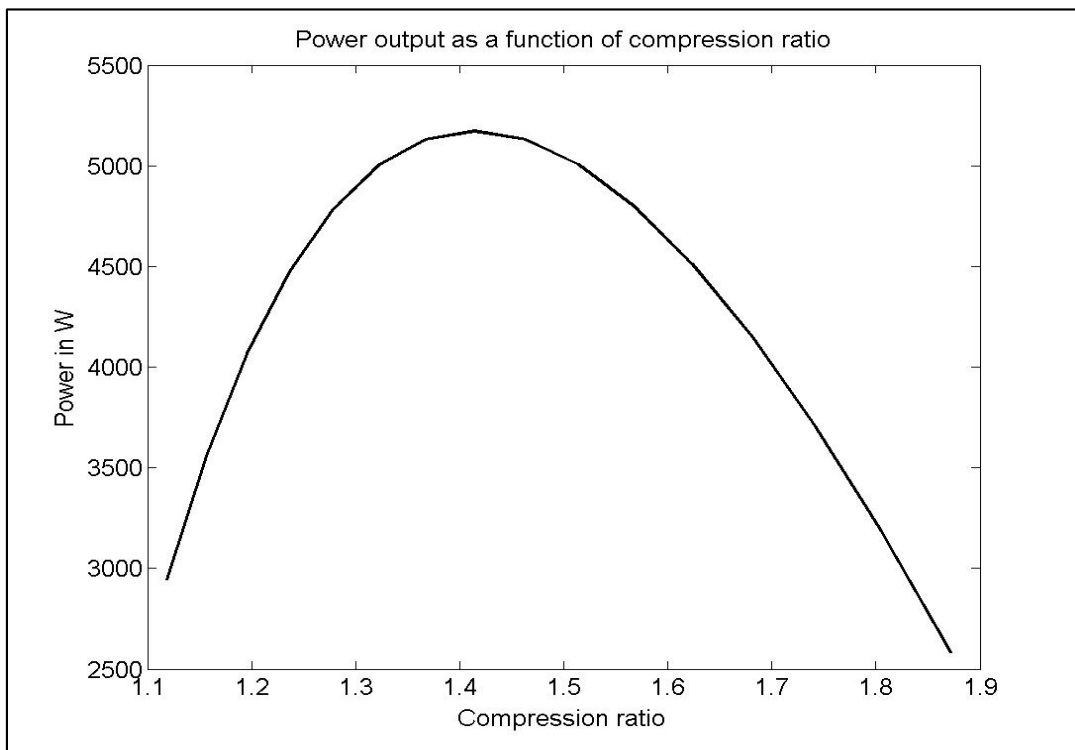


Figure 38: Compression ratio optimization for maximum power output

Now that the code has been validated by comparison with GPU-3 characteristics, a parametric study for the prototype to be manufactured has been presented below. The design of prototype proceeds simultaneously with the study for an optimum design by the end of the study. To start with, the Beale equation is used. This is a simple first order equation utilizing statistical data to determine basic engine parameter that which could be either working volume, operating frequency or working pressure. All variables other than the one to be determined have to be assigned a value. The approximate equation for power output of a Stirling engine is given in the book on Stirling engines by Walker (16). It was developed by William Beale, using statistical data of numerous Stirling engines manufactured over the years, and is given as

$$P = 0.015 f V p$$

Where,

P= Power output, in W

f= Frequency of operation of engine, in Hz

V= total working volume of the engine, in cm³

p= mean pressure inside engine, in bar

The working fluid will be helium gas. The targeted power output for the test case will be 500W.

- Working gas initial pressure = 7 bar.
- Cold end working volume = $740/3 = 246.67\text{cm}^3$. (from above formula)
- Displacer hot end and cold end volume = 120 cm^3 .
- Hot end temperature = 800K.
- Cold end temperature = 300K.
- Regenerator effectiveness = 1 (unless specified)

Now, using this equation and assuming the engine frequency of 15Hz (900 rpm), and mean pressure of 3 bar, the required working volume equals 740 cm^3 to produce a work output of 500W. The advantage of this equation is that it does not depend on the working fluid or the engine hot end and cold end temperatures. But the accuracy of the output of this equation is definitely constrained by the operating temperatures and working fluid. This equation works best for medium temperature differential (which is our case). The actual power output may deviate depending upon accuracy of manufacturing and how well the engine has been designed. An engine that is designed optimally and manufactured well may give higher power output than that predicted by above equation. So the above equation gives

a rough idea of what power output is to be expected, and gives something to start with.

Now the basic engine parameters have been defined, the mean pressure (which is assumed), the operating frequency (again this is assumed and ultimately will be decided based upon the outcome of the dynamic analysis of the engine) and the working volume which was determined to be equal to 740cm^3 . These values would be used in the test case using the thermodynamic adiabatic analysis of the engine. Also the hot end and cold end temperatures are assumed to be 600°C (873K) and 50°C (323K) respectively. These parameters are sufficient to complete the analysis. Of course the design process is iterative and needs tweaks to the above parameters till the best possible combination and optimal performance is obtained. Here a parametric study will come in handy to see the response of engine performance (mainly work and efficiency) to change in design parameters. The mechanical dimensions of the engine will also undergo an iterative design process. We will initially assume certain engine cylinder diameter, length to diameter ratio, wall thickness, displacer diameter, displacer length to diameter ratio, power piston diameter, power piston diameter ratio, engine clearance height at hot end and cold end and finally the regenerator volume. These look like a lot of unknowns but actually they are not. Almost all of them depend on each other and are constrained

by the working volume of 740cm³. So actually only a couple of important dimensions can be varied and the other dimensions will automatically adjust themselves.

Some remarks before proceeding-

- The results obtained are using the adiabatic analysis code.
- Viscous and frictional losses within the engine are not considered in the adiabatic analysis.
- The engine output behavior is studied by varying one or two parameters at a time.
- The engine operating temperature is 800K at hot end and 300K (actually should be around 320K). For these temperatures the maximum efficiency is-

$$\eta_{\max} = (1 - (300/800)) * 100 = 62.5\%.$$

- Hence the maximum adiabatic analysis efficiency for ideal case should be around 55-58%.
- L/D ratio for displacer will be 0.5 unless otherwise specified.
- Displacer height will be 8cm.
- Displacer diameter will be 6.75cm and stroke will be 3.375cm unless exception is specified.

- Power piston diameter will be 8 cm and stroke will be 2.52cm unless specified separately.
- Clearance gap for displacer at hot and cold ends will be 5mm unless varied for study.
- Also the results are for a single cylinder only. In our design we will be using 3 such modules.
- The working fluid assumed is Helium.
- The ratios of volumes of hot end heat exchanger, cold end heat exchanger and regenerator are constant at all times.

Variation of regenerator effectiveness:

The effectiveness of regenerator shall be varied while keeping other parameters constant.

The result for this is shown below,

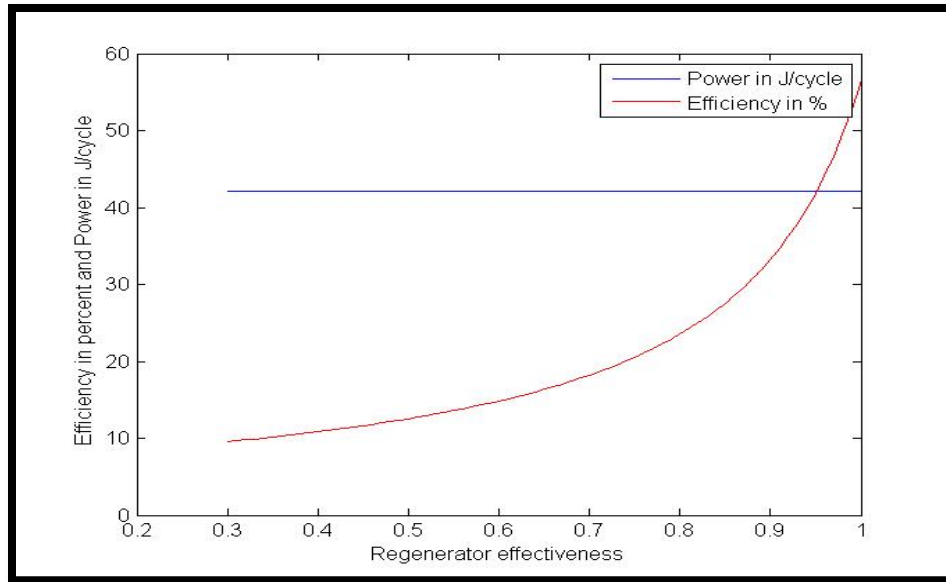


Figure 39: Power output and efficiency versus regenerator effectiveness

Observations-

- Regenerator effectiveness does not affect engine power output. This is expected since the power output will depend only on the engine pressure and working volume which is constant.
- The regenerator effectiveness affects efficiency of the engine. The steep slope signifies the role of regenerator effectiveness towards the efficiency of the engine and suggests that it is one of the critical parameters for achieving high efficiency. The behavior is exactly what is suggested in literatures.

Variation of phase angle between displacer and power piston:

The phase angle will now be varied while keeping other parameters constant. Note that the curves are specific to the engine dimensions and operating parameters. However the nature of this curve shall be more or less the same for all Stirling engine configurations since they work on the same fundamental Stirling cycle. The optimum phase angle is calculated based on thermodynamic analysis alone.

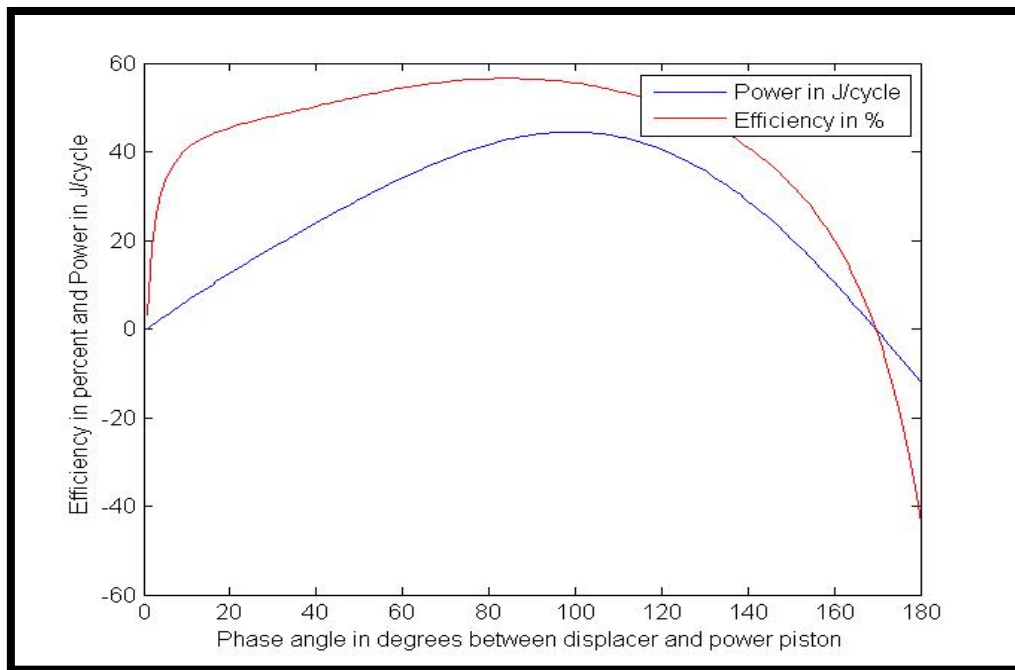


Figure 40: Power and efficiency versus phase angle

Observations:

- As suggested in various literature, the best possible power output is for phase angle between 80° to 100°.

- The engine specific efficiency curve shows best possible efficiency for the same phase angle range. However if we keep the other engine parameters flexible, we will find maximum efficiency for lower phase angles.

Variation of L/D ratio and compression ratio of engine.

Now keeping the working volumes and other parameters mentioned below same, we will vary compression ratio and L/D ratio for engine. A careful choice of compression ratio should be made as higher compression ratio results in difficulty in starting and sustaining if not designed accurately.

Compression ratio: is the ratio of maximum volume to minimum volume in the engine during the cycle.

L/D ratio: ratio of displacer/piston stroke to displacer/piston diameter.

We assume same L/D for displacer and piston.

- Working gas initial pressure = 7 bar.
- Cold end working volume = $740/3 = 246.67\text{cm}^3$.
- Displacer hot end and cold end volume = 120 cm^3 .

- Hot end temperature = 800K.
- Cold end temperature = 300K.
- Regenerator effectiveness = 1.

The result below shows the significant effect of compression ratio of the Stirling engine on the power output and thermal efficiency. The number just above the curves is the value of length to diameter ratio for the respective curve.

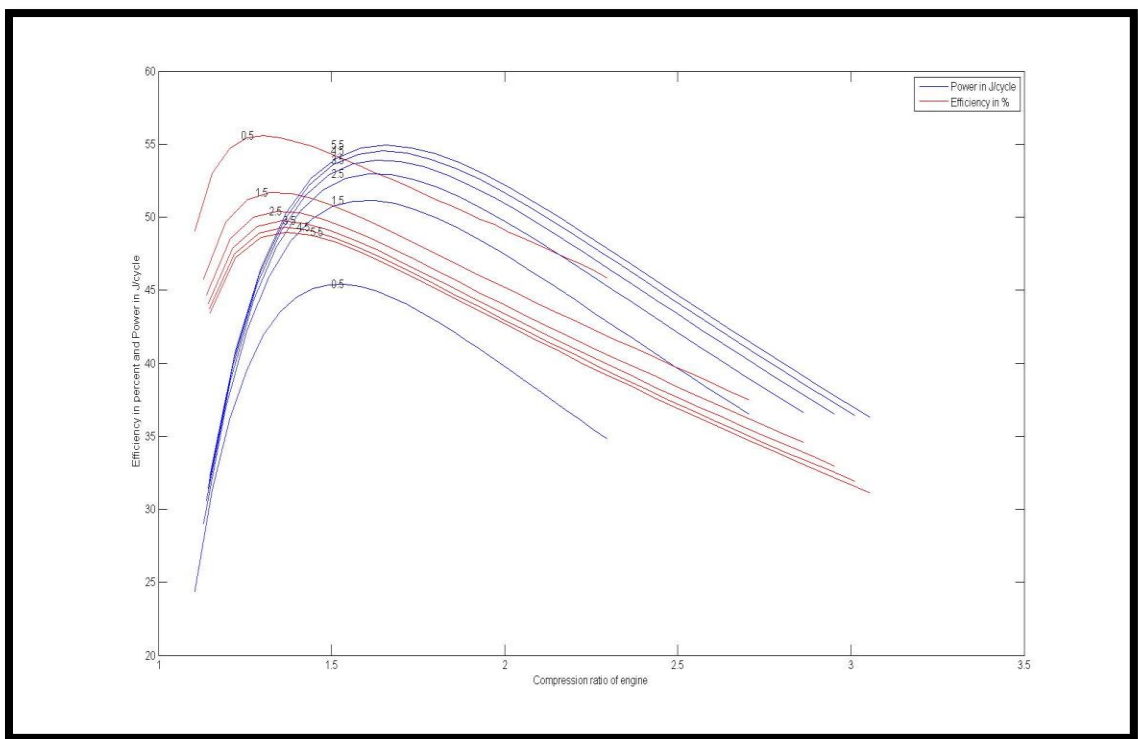


Figure 41: Power and efficiency versus comp. ratio for variable L/D

Observations-

- The number next to the curve is the L/D ratio for that curve.
- As we increase compression ratio from 1 to higher values, power output increases and then drops down.
- Similar behavior is observed for efficiency vs compression ratio curve.
- Now the power output increases with increase in L/D ratio, but the efficiency decreases.
- Again note these are engine specific results for our engine dimensions.

Variation of dead volume:

We now keep all our parameters fixed except the clearance above and below displacer that is nothing but the dead volume.

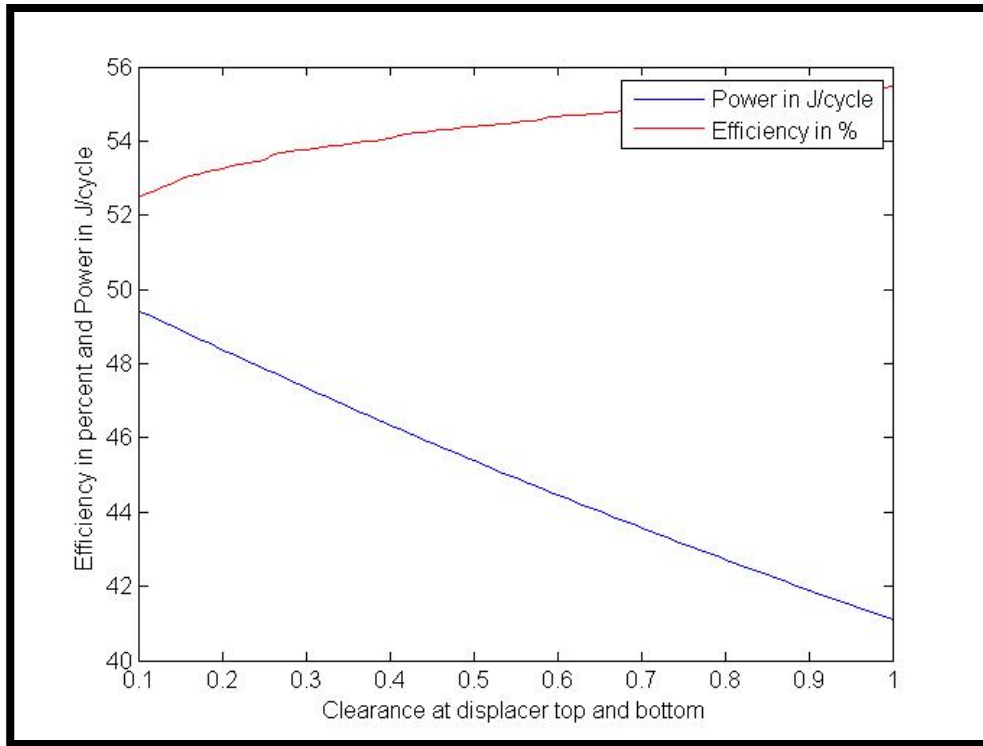


Figure 42: Power and efficiency versus clearance height

Observations-

- Clearance ratio does not significantly affect the efficiency of the engine.
- But power output significantly decreases as the clearance ratio increases. This is in agreement with theory which says that dead volume does not contribute to efficiency but reduces power output.

Some plots for the engine with all parameters kept constant

We will plot the work output, heat input, heat rejected, regenerator heat versus the crank/cycle angle. The regenerator heat initially increases

signifying heat absorption from the hot working fluid, and then decreases to zero signifying heat rejection to the cold working fluid. The net regenerator heat will remain zero as we have assumed perfect regeneration. The work output initially is negative which means work for compression has been pumped into the system. Eventually the expansion work which is greater than the compression work takes over and net positive work output is obtained.

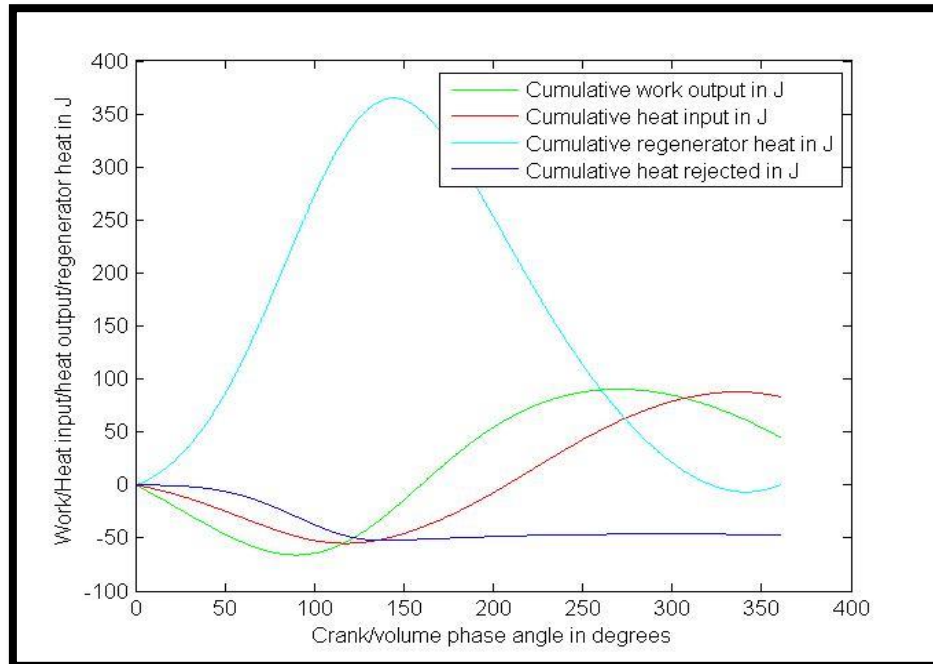


Figure 43: Work and heat in the cycle versus volume phase angle

A comparison of the nature of this plot can be made with the one provided by Urieli and Berchowitz in their analysis (14) of the GPU-3 Stirling engine. The plot reproduced from their work is shown below,

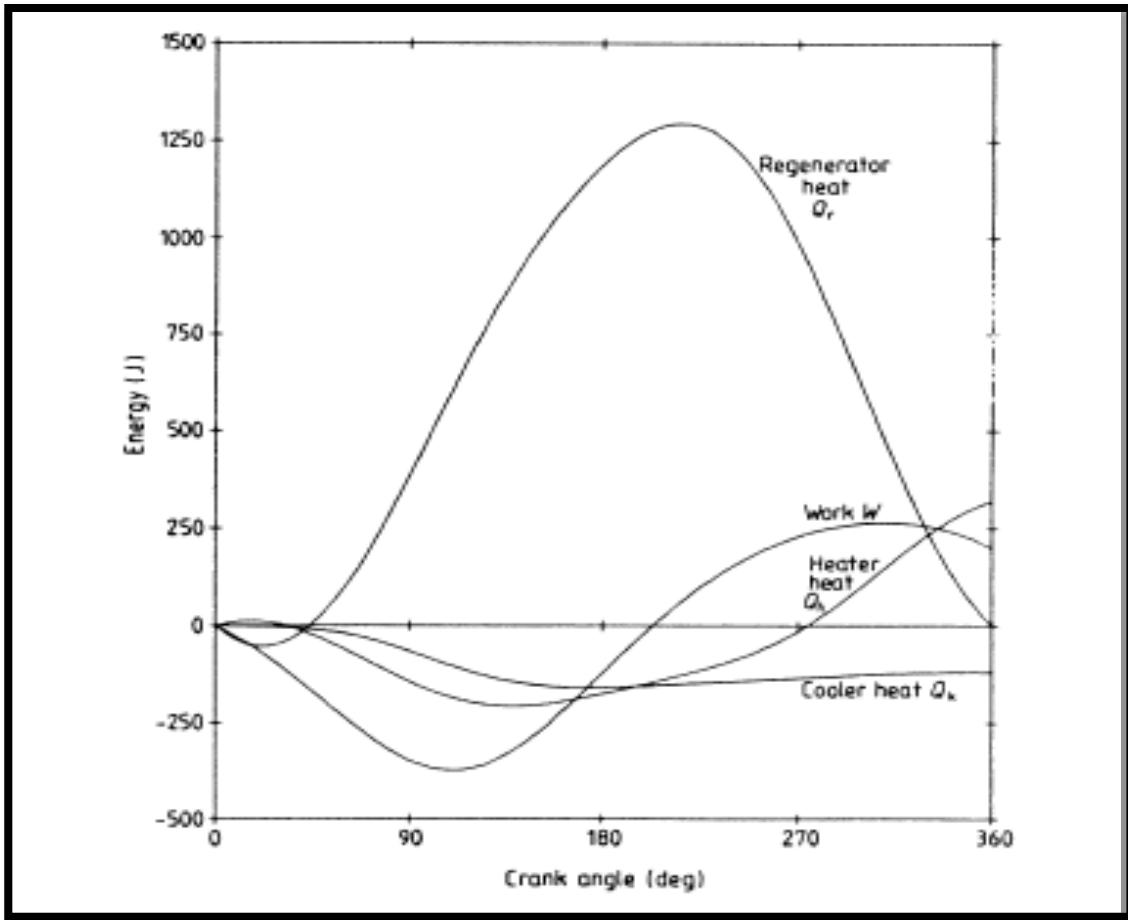


Figure 44: Work and heat in a cycle for GPU-3

The comparison shows that the nature of the two plots are in agreement even though the magnitude of the quantities are different. Urieli and Berchowitz used adiabatic analysis (14) for the General Motors GPU-3 engine and the above plot is one of the outputs of their analysis. The agreement between the two plots validates the adiabatic analysis presented and the Matlab code developed for performing the analysis.

Manufacturing of the free piston prototype

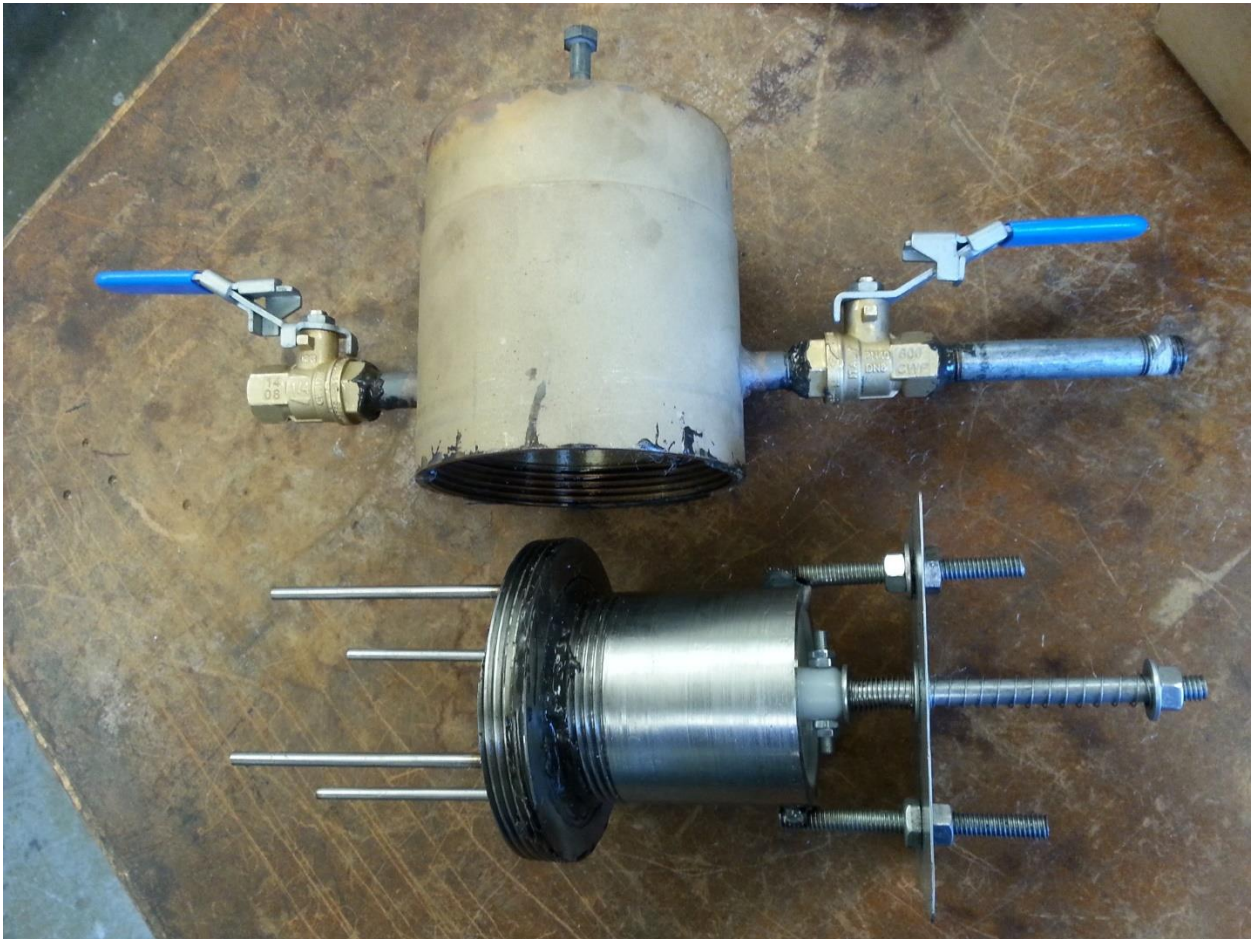


Figure 45: Displacer and power piston chambers

The figure shows the top and bottom half of the first prototype of the free piston Stirling engine. The two halves would be threaded together for final assembly. The brass chamber forms the top half that houses the displacer and the bottom cylinder has the working piston reciprocating within an acetyl lining. The prototype was entirely manufactured in the Mechanical engineering department machine shop at the University of Washington.



Figure 46: Displacer chamber with regenerator

The regenerator is wound around the displacer as seen. The regenerator is fine aluminum mesh. The displacer reciprocates axially on a shaft attached at the center of the displacer chamber. The displacer movement is constrained at the bottom by attaching a nut to the bottom end of the shaft. The shaft length and the position of the nut determines the maximum displacer stroke. Springs are attached on the top and bottom of the displacer to store energy and maintain the displacers reciprocating motion.

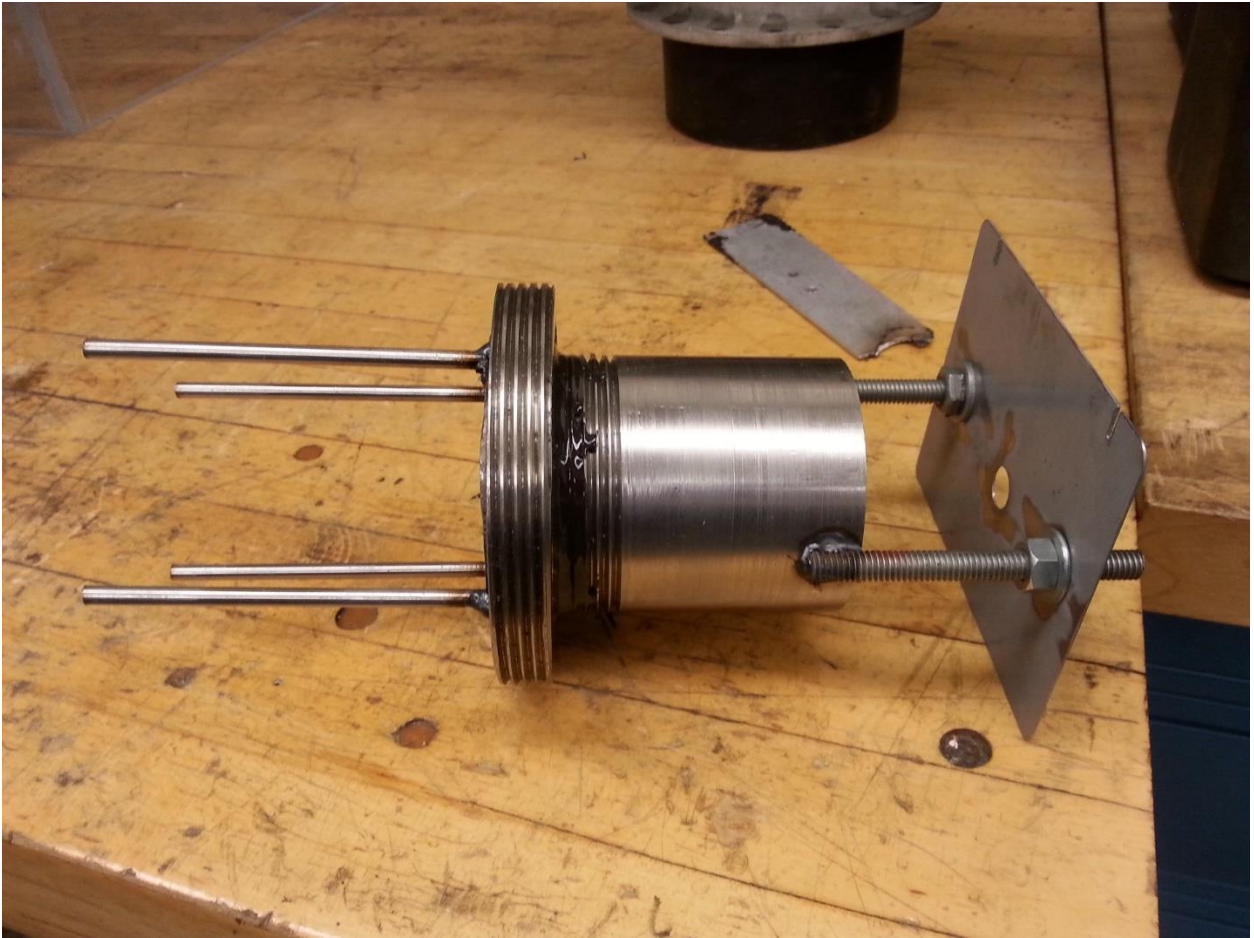


Figure 47: Working piston chamber with projections to support displacer
The working piston chamber has an acetyl lining and acetyl piston sliding inside it to reduce weight. The cylinders are threaded for flexibility and to easily make changes to the engine whenever required. Silicon based sealants are used to ensure that the threaded joints are sealed during operation. The four stainless steel projections help in positioning the displacer and also in coiling the regenerator mesh around the displacer area. The plate at the bottom of the working piston is used to adjust the working piston stroke and also supports the working piston springs.

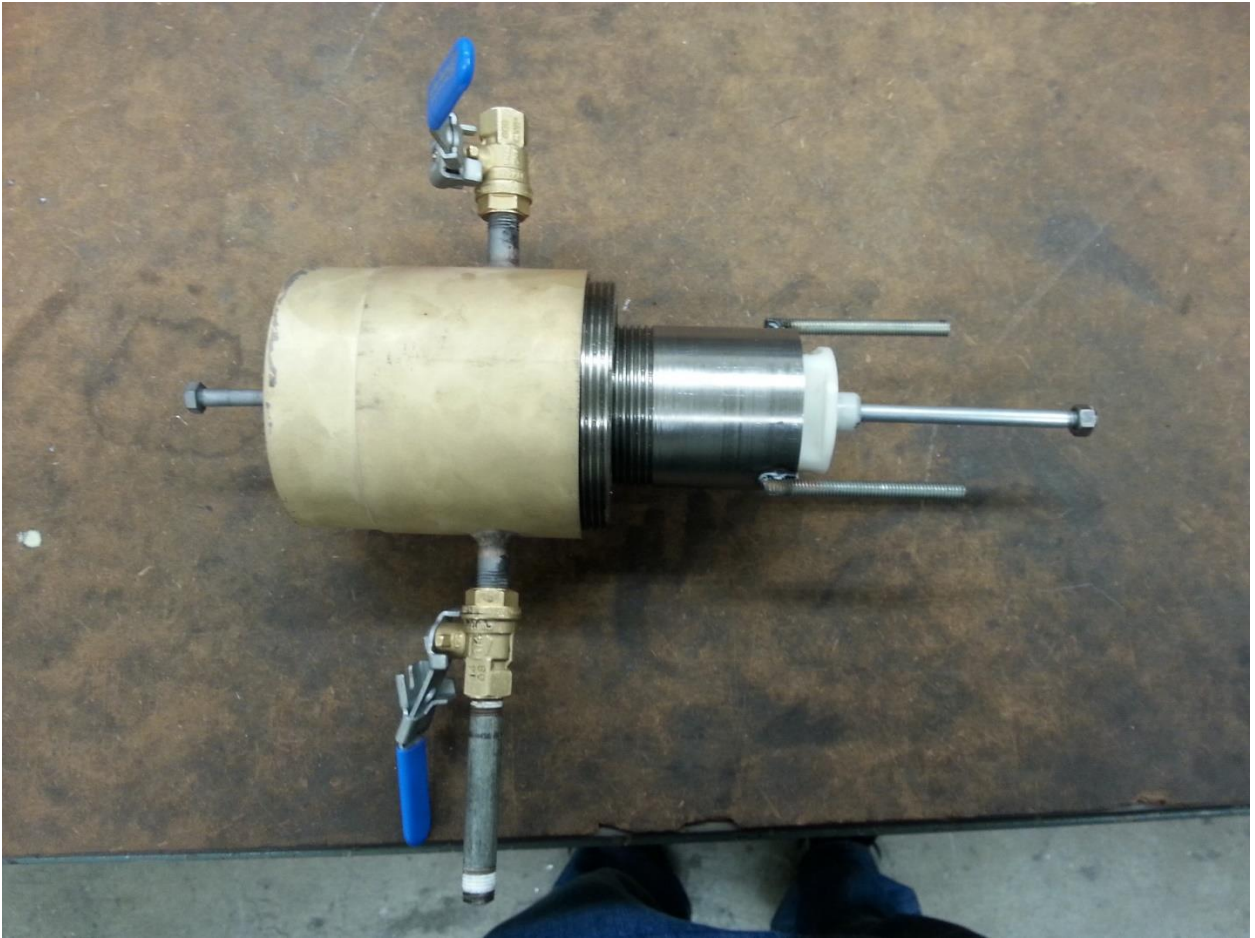


Figure 48: Final assembly of the free piston engine

Bibliography

1. **BP.** *Statistical Review of World Energy.* 2014.
2. **Roger, Sedjo.** *Comparative Life Cycle Assesments: Carbon Neutrality and Wood Biomass Energy.* Washington DC : s.n., 2013.
3. **Titiaan Palazzi, Amory Lovins.** *Micropower Database 2014 .* s.l. : Rocky Mountain Institute, 2014.
4. **Kim, Seon-Young.** *Specific power estimations for free piston Stirling engines.* San Diego : IECEC, 2006.
5. **Koornneef, Joris.** *Development of fluidized bed combustion- An overview of trends, performance and costs.* The Netherlands : Science Direct, 2006.
6. **Curkeet, Rick.** *Wood combustion basics.* 2011.
7. **Nayak, Amrit Om.** *Holistic Modeling, Design & Analysis of Integrated Stirling and Auxiliary Clean Energy Systems for Combined Heat and Power Applications.* Seattle : s.n., 2015.
8. **Mason, larry.** *Wood to energy in Washington: Imperativs, Opportunities and Obstacles to progress.* Seattle : s.n., 2009.
9. **Klett, James.** *High thermal conductivity, mesophase pitch derived carbon foams.* Ohio : ORNL.

10. **D.G.Thombare.** *Technological development in the Stirling cycle engines.* Lonere, India : Science Direct, 2006.
11. **Martini, William.** *Stirling engine design manual.* 1983.
12. **Martinez, Jose.** *Some mathematical models to describe the dynamics behaviour of the B-10 free piston Stirling engine.* Columbus : s.n., 1994.
13. **Hirata, Koichi.** *Schmidt theory for stirling engines.* s.l. : National Maritime Research Institute .
14. **Berchowitz, Urieli and.** *Stirling cycle engine analysis.* 1995.
15. **Timoumi, Yousef.** *Design and Perfomance Optimization of GPU-3 Stirling Engine.* Monastir : Science Direct, 2007.
16. **G.Walker.** *Stirling Engines.*

Appendix

Matlab program for isothermal analysis

```
clc;
```

```
clear all;
```

```
%approach 1: NASA's numerical integration method
```

```
%Nomenclature and units :
```

```
%W=work in J
```

```
%HD=hot end dead volume in cm3
```

```
%CD=cold end dead volume in cm3
```

```
%VL=hot end live volume in cm3
```

```
%VK=cold end live volume in cm3
```

```
%VP=power piston live volume in cm3
```

```
%RD=regenerator dead volume in cm3
```

```
%TH=hot end temperature in K
```

```
%TC=cold end temperature in K
```

```
%TR=regenerator mean temperature in K
```

```
%M=moles of gas in gmol
```

```
%R=universal gas constant
```

```
%AL=phase angle (to be used in radian)
```

```

%F=crank angle (to be used in radian)

%F1=crank angle in degrees

%HN=hot end instantaneous live volume in cm3

%CN=cold end instantaneous live volume in cm3

%VN=total instantaneous volume of gas in engine in cm3

%PN=instantaneous pressure of gas in engine in MPa

W=0;

HD=0;

CD=0;

VL=40;

VK=40;

VP=40;

RD=40;

TH=600;

TC=300;

TR=450;

M=1.265;

R=8.314;

AL=pi/2;

F(1)=0;           %Phase angle in radian

F1(1)=0;         %Phase angle in degrees

```

```

HN(1)=(VL/2)*(1-cos(0)); %hot end
volume at F=0
CN(1)=((VK/2)*(1+cos(0)))+(VP/2)*(1-cos(0-(pi/2)));
%cold end volume at F=0
VN(1)=HN(1)+CN(1)+RD; %total
end volume at F=0
PN(1)=(M*R)/((HN(1)/TH)+(CN(1)/TC)+(RD/TR));
%Pressure at F=0

for i=2:361
    F(i)=(i-1)*1*pi/180; %set
instantaneous crank angle in radian
    F1(i)=(i-1)*1; %calculate
crank angle in degrees
    HN(i)=(VL/2)*(1-cos(F(i)));
%calculate hot live volume
    CN(i)=((VK/2)*(1+cos(F(i)))+(VP/2)*(1-cos(F(i)-AL)));
%calculate cold live volume
    VN(i)=HN(i)+CN(i)+RD; %calculate
instantaneous total volume
    PN(i)=(M*R)/((HN(i)/TH)+(CN(i)/TC)+(RD/TR));
%calculate instantaneous pressure

```

```

    dv=VN(i)-VN(i-1); %calculate
change in volume

    W=W+((PN(i-1)+PN(i))/2*dv);

%calculate and accumulate instantaneous work; use average
pressure value for better accuracy

end

disp('Work per cycle in J by numerical integration :')

disp(W);

plot(F1,VN);

hold on;

plot(F1,HN,'-r');

hold on;

%plot(F1,CN,'-g');

figure

plot(VN,PN,'-g'); %plot the
cycle PV diagram

%Mort Mayer's relation for work per cycle

%X,Y,Z,XX and XY are values used in Mayers relation and are
defined as in code

%below

XX=(VP/2)+CD+(VK/2)+(RD/2);

```

```

XY=HD+(VL/2)+(RD/2);

X=XX+((TC/TH)*XY);

Y=(VL/2)*(1-(TC/TH))*sin(AL);

Z=(VP-(VL*(1-(TC/TH))*cos(AL)))/2;

W1=M*R*TC*pi*Y*VP/((Y^2)+(Z^2))*((X/sqrt((X^2)-(Y^2)-(Z^2)))-
1);

disp('Work per cycle in J by Mayers relation :');

disp(W1);

%Senft equation for work per cycle

%Here also X,Y,Z,XX and XY are terms used for convenience and
are defined as
%given in code below

PX=58.10; %Max pressure attained during each
cycle

AU=TC/TH;

VL=VK;

XX=(RD+HD+CD)/VL;

XY=VP/VL;

X=sqrt(((AU-1)^2)+(2*(AU-1)*XY*cos(AL))+(XY^2));

```

```

Y= (4*XX*AU/ (1+AU) ) +1+AU+XY;
Z=sqrt (1+ (XY^2) - (2*XY*cos (AL) ) ) ;
W2=pi* (1-AU) *PX*VL*XY*sin (AL) / (Y+sqrt ( (Y^2) - (X^2) ) ) * (sqrt ( (Y-
X) / (Y+X) ) ) ;
disp('Work per cycle in J as per Senft equation :');
disp(W2);
%Cooke-Yarborough equation

XX=VL+RD+ (VP/2) ;
XY= (RD/2) + (VK/2) + (VP/2) ;
Pmean=40.59; %mean pressure during cycle
W3=pi*Pmean/4*VL*VP* (TH-TC) *sin (AL) / (XX* (TC+ (XY/XX* (TH-TC) ) ) ) ;
disp('Work per cycle in J by Cooke-Yarborough relation :');
disp(W3);

```

Matlab code for adiabatic analysis

```
clear all;
```

```
clc;
```

```
%ADIABATIC ANALYSIS
```

```
%Nomenclature
```

```
% Ve(j,i)=Maximum Hot end volume
```

```
% Vhe=Hot end heat exchanger volume
```

```
% Vhd=hot end dead volume
```

```
% Vc(j,i)=Cold end volume
```

```
% Vc(j,i)e=cold end heat exchanger volume
```

```
% Vc(j,i)d=cold end dead volume
```

```
% Vd=cold end maximum displacer volume
```

```
% Vp=cold end maximum piston volume
```

```
% Vr=regenerator volume
```

```
% The=hot end heat exchanger temperature
```

```
% Tce=cold end heat exchanger temperature
```

```
% Tr=regenerator temperature
```

```
% Te=expansion space temperature
```

```

% Tc=compression space temperature

% me=expansion space mass
% meh=hot end heat exchanger mass
% mr=regenerator mass
% mc=compression space mass
% mec=cold end heat exchanger mass

% p=instantaneous pressure
% r=Co/Cv for the working gas
% R=gas constant;
%
% f=crank angle
% AL=phase lag

%Define constant values

R=2.0679*1000;      %Set the value of gas constant for your
working fluid
r=1.666666672;     %Set the value of ratio of specific heats
for your working fluid

```

```
Cp=5.1926*1000;      %Set the value of specific heat of working
fluid at constant pressure. Enter the value of specific heat
at the heater temperature
```

```
Cv=3.1156*1000;      %Set the value of specific heat of working
fluid at constant volume. Enter the value of specific heat at
the heater temperature
```

```
m=0.1;              %This crank angle resolution is optimum
when solving explicit relation for pressure
```

```
k=10;              %It is known that the convergence should
take around 5 iterations. However we set the array size of the
variables so that it can store up to 10 iteration data. It is
not advisable to keep increasing the array size with each
iteration because this will slow the computational speed.
```

```
AL=pi/180*90;      %Set the desired/design phase angle
between displacer and power piston
```

```
flag=0;            %flag will be set to 1 when the error
criterion is satisfied
```

```
%Set engine parameters
```

```

Vhe=input('Enter hot end heat exchanger volume in cm3: ');
Vce=input('Enter cold end heat exchanger volume in cm3: ');
Vr=input('Enter regenerator section volume in cm3: ');

%Set initial conditions

Th=input('Enter hot end heat exchanger temperature in K: ');
Tk=input('Enter cold end heat exchanger temperature in K: ');
Tr=(Th-Tk)/log(Th/Tk);

n=(360/m)+1;

%Initialize arrays to store variables

p=zeros(k,n);
p(1,1)=input('Enter the initial charging pressure in MPa: ');
Ve=zeros(k,n);
Vc=zeros(k,n);
v=zeros(k,n);
Te=zeros(k,n);
Tc=zeros(k,n);

Wl=zeros(k,n);

```

```

%Volume arrays

Vem=input('Enter expansion end working volume in cm3: ');
Vp=input('Enter compression end piston working volume in cm3:
');

Vcm=Vem;

%Vp=Vp-(Vem/2);

Vd=Vem+Vp;

Ved=30.52;

Vcd=28.68;

Ve(1,1)=(Vd/2*(1-cos(m*pi/180)));           %Start with displacer
at topmost position

Vc(1,1)=(Vd/2*(1+cos(m*pi/180))+Vp/2*(1-cos((m*pi/180)-
(AL)))));

Vpiston=zeros(k,n);

Vcompression=zeros(k,n);

v=zeros(k,n);

v(1,1)=Vc(1,1)+Ve(1,1)+Vr+Vhe+Vce;

v(2,1)=v(1,1);

%Mass arrays

```

```
Dmc=zeros(k,n);
```

```
%The following variables are nothing but the values of  
instantaneous mass flowing across
```

```
%control volumes
```

```
gAck=zeros(k,n);
```

```
gAkr=zeros(k,n);
```

```
gArh=zeros(k,n);
```

```
gAhe=zeros(k,n);
```

```
Dmce=zeros(k,n);
```

```
Dmr=zeros(k,n);
```

```
Dmhe=zeros(k,n);
```

```
%These are the instantaneous mass contents of each control  
volume
```

```
mce=zeros(k,n);
```

```
mhe=zeros(k,n);
```

```
mr=zeros(k,n);
```

```
me=zeros(k,n);
```

```
mc=zeros(k,n);
```

```
meact=zeros(k,n);
```

```
%Work and Heat arrays
```

```
DQk=zeros(k,n);
```

```
Qk=zeros(k,n);
```

```
DQr=zeros(k,n);
```

```
Qr=zeros(k,n);
```

```
DQh=zeros(k,n);
```

```
Qh=zeros(k,n);
```

```
DW=zeros(k,n);
```

```
%Other arrays
```

```
f=zeros(k,n);
```

```
fd=zeros(k,n);
```

```
dexp=zeros(k,n);
```

```
dcomp=zeros(k,n);
```

```
num=zeros(k,n);
```

```
den=zeros(k,n);
```

```
Dp=zeros(k,n);
```

```
carnot_efficiency=zeros(k,n);
```

```
instant_efficiency=zeros(k,n);
```

```
Tck=Tc(1,1);
```

```
The=Th;
```

```
term=r*((Vce/Tck)+(Vr/Tr)+(Vhe/The));
```

```

M= (p(1,1) * (Ve(1,1) + Ved) / R / Th) + (p(1,1) * (Vc(1,1) + Vcd) / R / Tk) + (p(1
,1) * Vr / R / Tr) + (p(1,1) * Vhe / R / Th) + (p(1,1) * Vce / R / Tk);

%constant mass of gas in engine

mr(1,1) = (p(1,1) * Vr / R / Tr);

mhe(1,1) = (p(1,1) * Vhe / R / Th);

mce(1,1) = (p(1,1) * Vce / R / Tk);

mc(1,1) = (p(1,1) * (Vc(1,1) + Vcd) / R / Tk);

% me(1,1) = M - (mr(1,1) + mhe(1,1) + mce(1,1) + mc(1,1));

Te(1,1) = Th;

Tc(1,1) = Tk;

j=0;

while flag<1

    j=j+1;

    Ve(j,1) = (Vd/2 * (1 - cos(m*pi/180)));

%Start with displacer at topmost position

%Initialize volumes, masses and temperature values

```

```

Vc(j,1)=(Vd/2*(1+cos(m*pi/180))+Vp/2*(1-cos((m*pi/180)-(AL)))));
Vpiston(j,1)=Vp/2*(1-cos((m*pi/180)-(AL)));
Vcompression(j,1)=Vd/2*(1+cos(m*pi/180));
v(j,1)=Vc(j,1)+Ve(j,1)+Vce+Vhe+Vr+Ved+Vcd;
mr(j,1)=(p(j,1)*Vr/R/Tr);
mhe(j,1)=(p(j,1)*Vhe/R/Th);
mce(j,1)=(p(j,1)*Vce/R/Tk);
mc(j,1)=(p(j,1)*(Vc(j,1)+Vcd)/R/Tc(j,1));
me(j,1)=M-(mr(j,1)+mc(j,1)+mhe(j,1)+mce(j,1));
Te(j,1)=p(j,1)*(Ve(j,1)+Ved)/R/me(j,1);
Tck=Tc(j,1);
The=Th;

```

```

for i=2:n

```

```

    fd(j,i)=i*m;
    f(j,i)=i*m*pi/180;
    Ve(j,i)=(Vem/2*(1-cos(f(j,i)))));
    dexp(j,i-1)=Ve(j,i)-Ve(j,i-1);
    Vc(j,i)=(Vd/2*(1+cos(f(j,i))+Vp/2*(1-cos(f(j,i)-AL)))));
    dcomp(j,i-1)=Vc(j,i)-Vc(j,i-1);
    Vcompression(j,i)=Vd/2*(1+cos(f(j,i)));
    Vpiston(j,i)=Vp/2*(1-cos(f(j,i)-AL));

```

```

v(j,i)=Vc(j,i)+Ve(j,i)+Vce+Vhe+Vr+Vcd+Ved;
num(j,i)=-r*p(j,i-1)*(((dcomp(j,i-1))/Tck)+(((dexp(j,i-
1))/The)))));
term=r*((Vce/Tck)+(Vr/Tr)+(Vhe/The));
den(j,i)=((Vc(j,i)+Vcd)/Tck)+term+((Ve(j,i)+Ved)/The);
Dp(j,i)=num(j,i)/den(j,i);

p(j,i)=p(j,i-1)+Dp(j,i);

Dmc(j,i)=(((p(j,i)*dcomp(j,i-
1))+((Vc(j,i)+Vcd)*Dp(j,i)/r)))/(R*Tck);
mc(j,i)=mc(j,i-1)+Dmc(j,i);
mr(j,i)=(p(j,i)*Vr/R/Tr);
mhe(j,i)=(p(j,i)*Vhe/R/Th);
mce(j,i)=(p(j,i)*Vce/R/Tk);
me(j,i)=M-(mc(j,i)+mr(j,i)+mhe(j,i)+mce(j,i));
meact(j,i)=p(j,i)*Ve(j,i)/R/Te(j,i-1);
error(j,1)=abs(me(j,i)-meact(j,i));

Tc(j,i)=p(j,i)*(Vc(j,i)+Vcd)/R/mc(j,i);
Te(j,i)=p(j,i)*(Ve(j,i)+Ved)/R/me(j,i);

Dmce(j,i)=mce(j,i)*Dp(j,i)/p(j,i);

```

```

Dmr(j,i)=mr(j,i)*Dp(j,i)/p(j,i);
Dmhe(j,i)=mhe(j,i)*Dp(j,i)/p(j,i);

gAck(j,i)=-Dmc(j,i);
gAkr(j,i)=gAck(j,i)-Dmce(j,i);
gArh(j,i)=gAkr(j,i)-Dmr(j,i);
gAhe(j,i)=gArh(j,i)-Dmhe(j,i);

if gAck(j,i)>0
    Tck=Tc(j,i);
    Tkr=Tk;
else
    Tck=Tk;
    Tkr=Tk;
end

if gAhe(j,i)>0
    The=Th;
    Trh=Th;
else
    The=Te(j,i);
    Trh=Th;
end

DW(j,i)=(p(j,i)+p(j,i-1))/2*(dcomp(j,i-1)+dexp(j,i-1));

```

```

W1(j,i)=W1(j,i-1)+DW(j,i);
DQk(j,i)=(Vce)*Dp(j,i)*Cv/R)-Cp*((Tck*gAck(j,i))-
(Tkr*gAkr(j,i)));
Qk(j,i)=Qk(j,i-1)+DQk(j,i);
DQr(j,i)=(Vr*Dp(j,i)*Cv/R)-Cp*((Tkr*gAkr(j,i))-
(Trh*gArh(j,i)));
Qr(j,i)=Qr(j,i-1)+DQr(j,i);
Qh(j,i)=W1(k,n)-Qk(k,n);
carnot_efficiency(j,i)=1-(Tc(j,i)/Te(j,i));
end
p(j+1,1)=p(j,n);
Tc(j+1,1)=Tc(j,n);
if j>2
    error(j,1:n)=p(j,1:n)-p(j-1,1:n);
    if max(abs(error(j,1:n)))<0.001
        flag=1;
    end
end
end
end
% fink=50*area/10000/15/M/4/5.19/1000;

```

```

% disp('Finkelstein number for the engine = ');
% disp(fink);
% clearance(1,temp1)=h;
% Power(1,temp1)=W1(k,n);
% efficiency(1,temp1)=(W1(k,n)/Qh(k,n))*100;
% temp1=temp1+1;

% figure
% plot(fd(k,1:n),Ve(k,1:n),'-m','linewidth',2);
% hold on;
% plot(fd(k,1:n),Vc(k,1:n),'-r','linewidth',2);
% hold on;
% plot(fd(k,1:n),Vpiston(k,1:n),'-k','linewidth',2);
% hold on;
% plot(fd(k,1:n),v(k,1:n),'-b','linewidth',2);
% hold on;
% legend('expansion working volume','compression working
volume','power piston working volume','total engine volume');
% xlabel('Crank angle in degree');

```

```

% ylabel('Volume in cm3');

% %

% %

% figure;

% plot(fd(k,1:n),me(k,1:n),'-m','linewidth',2);

% hold on;

% plot(fd(k,1:n),mhe(k,1:n),'-r','linewidth',2);

% hold on;

% plot(fd(k,1:n),mr(k,1:n),'-k','linewidth',2);

% hold on;

% plot(fd(k,1:n),mce(k,1:n),'-b','linewidth',2);

% hold on;

% plot(fd(k,1:n),mc(k,1:n),'-c','linewidth',2);

% hold on;

%

plot(fd(k,1:n),mc(k,1:n)+me(k,1:n)+mhe(k,1:n)+mce(k,1:n)+mr(k,
1:n),'-g');

% legend('hot working volume','hot heat
exchanger','regenerator','cold heat exchanger','cold working
volume','Total gas mass in engine');

% xlabel('Crank angle in degrees');

% ylabel('Mass in kg');

%

```

```

% figure;
% plot(fd(k,1:n),p(k,1:n),'linewidth',2);
% xlabel('Crank angle in degrees');
% ylabel('Pressure in MPa');
%
%
% figure;
% plot(v(k,1:n),p(k,1:n),'linewidth',2);
% xlabel('Volume in cm3');
% ylabel('Pressure in MPa');
%
%
%
% figure;
% plot(fd(k,1:n),gAck(k,1:n),'-r','linewidth',2);
% hold on;
% plot(fd(k,1:n),gAkr(k,1:n),'-b','linewidth',2);
% hold on;
% plot(fd(k,1:n),gArh(k,1:n),'-c','linewidth',2);
% hold on;
% plot(fd(k,1:n),gAhe(k,1:n),'-g','linewidth',2);
% xlabel('Crank angle in degrees');
% ylabel('mass flow in kg');

```

```

% legend('Mass flow rate between cold end working volume and
heat exchanger','Mass flow rate between cold end heat
exchanger and regenerator','Mass flow rate between regenerator
and hot end heat exchanger','Mass flow rate between hot end
heat exchanger and working volume');

%

% %

disp('Compression ratio for the engine = ');
disp(max(v(j,1:n))/min(v(j,1:n)));
Qh(j,n)=Wl(j,n)-Qk(j,n);
disp('Heat given per cycle in J = ');
disp(Qh(j,n));
disp('Heat rejected per cycle in J = ');
disp(Qk(j,n));
disp('Regenerator net heat per cycle in J = ');
disp(Qr(j,n));
temp=(Wl(j,n)+Qh(j,n)+Qk(j,n))/2;
disp('Work output per cycle in J = ');
disp((Wl(j,n)));
disp('Efficiency of the engine in percentage = ');
disp((Wl(j,n)/Qh(j,n))*100);
disp('Power output for a 41.72 Hz operating frequency in W =
');

```

```

disp(W1(j,n)*16.67);

disp('Heat given per cycle in W = ');

disp(Qh(j,n)*16.67);

disp('Heat rejected per cycle in W = ');

disp(Qk(j,n)*16.67);

% %

% figure;

% plot(fd(k,1:n),Te(k,1:n),'-r','linewidth',2);

% hold on;

% plot(fd(k,1:n),Tc(k,1:n),'-c','linewidth',2);

% xlabel('Crank angle in degrees');

% ylabel('Temperature in K');

% legend('Expansion space temperature','Compression space
temperature');

%

disp('Mean operating pressure for the engine= ');

disp(mean(p(j,1:n)));

plot(fd(j,2:n),carnot_efficiency(j,2:n)*100);

%

% figure;

% plot(fd(k,1:n),DW(k,1:n),'-k','linewidth',2);

```

```

% xlabel('Crank angle in degrees');
% ylabel('Instantaneous work in J');
% figure;
% plot(fd(k,1:n),Wl(k,1:n),'-g');
% hold on;
% plot(fd(k,1:n),Qh(k,1:n),'-r');
% hold on;
% plot(fd(k,1:n),Qr(k,1:n),'-c');
% hold on;
% plot(fd(k,1:n),Qk(k,1:n),'-b');
% xlabel('Crank angle in degrees');
% ylabel('Heat/Work in J');
% legend('Work output','Heat input','Regenerator heat','Heat
rejected');

```